

# An overview of preparation and characterization of solid binary system and its application on transdermal film with variation of plasticizers

Nancy Kahali\*<sup>1</sup>, Jasmina Khanam<sup>1</sup>, Himadrija Chatterjee<sup>1</sup>

<sup>1</sup>Department of Pharmaceutical Technology, Jadavpur University, India

Chemotherapy induced nausea and vomiting (CINV) and post-operative nausea and vomiting (PONV) is a problem, often occurs in patient. In spite of high bioavailability, the demerits such as: hepatic first pass metabolism and invasive nature of oral and parenteral dosage forms can be avoided with anti-emetic therapy of transdermal device. The major objective of the present study is to modify the hydrochloride (HCl) form of Ondansetron (OND) to the base form followed by improvement of solubility and permeability of OND by employing solid dispersion (SD) loaded patches. Preformulation study, as observed, begins with an approach to enhance solubility of OND by SD technique choosing different carriers. The choice of carriers was rationalized by phase solubility study. Several combinations of transdermal films were prepared with pure drug, carriers and SDs with plasticizer Ka values of OND-HP $\beta$ CD binary system were found lower (54.43 to 187.57 M<sup>-1</sup>) than that of OND-PVP K-30 binary system (1156.77 to 12203.6 M<sup>-1</sup>). The drug content of SDs and patches were found satisfactory. Better permeation rate (236.48 $\pm$ 3.66  $\mu$ g/3.935 cm<sup>2</sup>) with promising flux enhancement (8.30 fold) was found with DBP loaded SD patch (P6\*). Hence, enhancement of solubility and permeability of P6\* ensures that it can successfully enhance the bioavailability.

**Keywords:** Ondansetron. Solubility. Inclusion complex. Permeation. Transdermal film.

## INTRODUCTION

Transdermal Drug Delivery (TDD) is undoubtedly an eloquent well-renowned dosage system developed as a drug laden gel or film that delivers the drug into the skin to reach systemic circulation by active or passive diffusion/permeation. Transdermal patches govern the transportation of drugs at a controlled manner by exerting a proper hydrophilic-lipophilic polymer mixture (Chien, 1987; Mukherjee *et al.*, 2005; Walters, 1999). The drug may either be loaded in matrix of a polymeric film or accumulated in a reservoir that requires porous release membrane (Ghanghoria *et al.*, 2013).

As because stratum corneum is a biological hindrance towards entry of molecules from the outer environment,

requisite drug molecules require verification on characteristics of drug and skin in times of preformulation study (Alany, 2017). In order to overcome the constraint of barrier mechanism to some extent, permeation enhancer requires to be incorporated. To avoid the brittleness of the film and to improve the smoothness of patch, addition of plasticizer is necessary (Loftsson, Masson, 2001).

Transdermal Drug Delivery System (TDDS) is a covenant route for drug delivery, generally applied in the treatment of local skin disorders such as: acne and several types of wounds (Guy, Green, Kealey, 1996; Ravikumar *et al.*, 2017). Apart from these, various other diseases are treated by transdermal route such as- Parkinson's disorder, Alzheimer's disease, motion sickness, hormone replacement therapy etc. It is to be mentioned that TDDS had its development in 1970 and the first transdermal patch of scopolamine had got its approval from United States Food and Drug Administration (USFDA) in 1979 for the treatment of motion sickness (Alany, 2017; Ahad

\*Correspondence: N. Kahali. Department of Pharmaceutical Technology, Jadavpur University, India. Phone: +918013613230. kahalinancy@gmail.com. jasminakhanam@gmail.com. himadrijabuuiya@gmail.com. ORCID ID: 0000-0002-9878-4792

*et al.*, 2015). Afterwards nitroglycerine patch was made available in the market for the management of Angina pectoris (Ahad *et al.*, 2010).

Ondansetron (OND), a selective 5-hydroxytryptamine (serotonin) receptor antagonist, is generally used in the prophylaxis of nausea and vomiting. Patients experiencing chemotherapy/radiotherapy usually encounters emesis (Khan *et al.*, 2007). It is absorbed effectively and can produce hepatic first-pass metabolism (Hassan *et al.*, 2009). Approximately 59% OND is bioavailable when administered by an oral route (Salem, Lopez, Galan, 2001). For transdermal route OND is consider as a good candidate because of its low molecular mass (293.36 g/mol), low dose efficacy and satisfactory log P (1.8-2.56) value (Prausnitz, Langer, 2008, Subedi *et al.*, 2010).

It is highly expedient and necessary also to develop a transdermal formulation in order for overcoming CINV and to make anti-emetic therapy an effective approach. For enhancement of permeation rate of the drug, some alterations to this respect are of course, necessary. The first step that is to be adopted is to use OND (base form) and the second one is to prepare solid dispersions (SDs) with it to quicken the solubility of the drug. Amongst many formulation approaches (Wu *et al.*, 2012) one that has been most successfully utilized is SD technique because it helps to increase solubility of poorly aqueous soluble drugs and also because it is easier to develop as it is cost effective. Innumerable methods have so far been adopted to prepare amorphous SDs, e.g. solvent evaporation, spray drying, kneading, freeze drying, hot-melt extrusion (Kalimuthu, Khanam, 2014).

The application of SDs in many research in transdermal devices, gels, micro-emulsions, was reported earlier (Palem *et al.*, 2013; Jana *et al.*, 2014; Desai, 2004). The development of SDs by kneading technique with PVP K-30 and HP $\beta$ CD to augment the solubility as well as dissolution rate with respect to celecoxib was established by Soliman and his co-workers. What they observed was that the kneaded SDs, after assimilation with o/w cream, enhanced the permeation rate to rabbit skin higher than that of pure celecoxib (Soliman *et al.*, 2011).

The purpose of the present study is to develop SD by using two different carriers like HP $\beta$ CD and PVP K-30 and incorporation of prepared SD into transdermal device

for the enhancement of dissolution rate, permeability as well as bioavailability (Di, Kerns, 2016). The objectives of the proposed work can be summarized as follows: a) Modification of OND from HCl to base form, b) To ensure the complexation ability of drug and carrier by phase solubility study c) Preparation of SDs and ascertainment of solubility of the drug, c) To perform in-vitro release and ex-vivo permeation studies of pure and SD loaded patches d) To characterize SDs and optimized patch. It is to be noted that these steps in the development of transdermal device with SD have not been reported as yet.

## MATERIAL AND METHODS

### Material

Polyvinyl pyrrolidone (PVP K-30), Hydroxypropyl beta cyclodextrin (HP $\beta$ CD) were purchased from Loba Chemie, Mumbai and Tokyo Chemical Industry Co. Ltd. Tokyo, Japan respectively. Ethyl cellulose (EC) was obtained from Sigma Aldrich Chemicals and Hydroxypropyl methyl cellulose E-15 (HPMC) was produced from Colorcon Asia Pvt. Ltd. Goa, India. Dibutyl phthalate (DBP) and polyethylene glycol 4000 (PEG) were procured from Merck specialities Pvt. Ltd. Mumbai, India. Ondansetron hydrochloride (OND HCl) and chloroform were obtained from Yarrow Chem. India. Release liner (Fluoropolymer 1022), adhesive (CoTran9697 non-woven polyurethane tape) and backing layer (SCOTCHPAK 9733) were procured from 3M Drug Delivery U.S.A. Cellophane membrane was procured from Sigma Aldrich Pvt. Ltd. All the chemicals used in this work are of analytical grade.

### Methods

#### *Modification of Ondansetron hydrochloride (OND HCl) to base (OND) form*

Known quantity (0.175 gm) of OND HCl was weighed and dispersed uniformly with required volume double distilled water (DDW). Sodium hydroxide solution (1 M NaOH) was then added to the drug solution to make it alkaline. Precipitate occurred during the addition of 1 M

NaOH is filtered through Whatman filter paper (150 mm pore size). The precipitate was allowed to wash repeatedly to eliminate excess amount NaOH and dry in a hot air oven at 50°C. The precipitate was allowed to wash repeatedly to eliminate excess amount NaOH. The washed solution was further treated with 1 M NaOH to check the presence of excess amount of NaOH in precipitate. The presence of excess amount of NaOH was confirmed if the washed solution forms turbidity after treatment of 1 M NaOH. The precipitate was rinsed with DDW until transparent solution was obtained. The precipitate was then allowed to dry in a hot air oven at 50°C. The dried mass was further cooled and required volume of boiled acetone was added (when reached its boiling point at 56°C) to the solid mass with constant stirring. The solution of drug was filtered for the removal of impurities. The solution was cooled and subsequently kept into refrigerator. Crystal produced after freezing was dried in a hot air oven at 50°C. After that the dried mass was stored for further application (Kahali, Khanam, 2018).

#### *Ascertainment of physicochemical properties of OND*

##### *Saturation solubility study*

The study was conducted by taking an excess amount of OND in graduated stopper test tubes with 5 mL DDW (pH 6.0), phosphate buffer pH 7.4 and pH 6.8 media. Then the test tubes were placed into water bath for 24 h at 37 ± 0.5°C and shuddered properly in regular intervals till the equilibrium is not attained. The content present in test tubes was centrifuged and filtered properly (by using Whatman filter paper, pore size 11 µm). After that desirable dilutions had been made. Finally, the absorbances were taken at λ<sub>max</sub>248 nm spectrophotometrically.

##### *Partition coefficient determination*

Measurement of partition coefficient is the most crucial side in this study because drug absorption is a general mechanism of passive diffusion. This mechanism solely depends on the partition coefficient of drug. The partition coefficient of drug is assessed by taking 10

mg OND and its SDs containing equal volume (15 mL each) of water and n-octanol in a separating funnel. Before addition of drug, two phases were allowed to get saturated by shaking (8 h) in a mechanical shaker. After that OND is added to the solution mixture and again shaking was done for 24 h in the same way. Then the funnel with mixture was left for 10 min to separate the mixture into two distinct layers. The aqueous phase (water) was collected and suitable dilutions were made and analyzed under UV-spectrophotometer. The same method was adopted with phosphate buffer pH 7.4 and n-octanol (Moldoveanu, David, 2015). The experiment was repeated thrice at 25 ± 0.5°C. The partition coefficient of OND was constituted by the following equation:

##### *Phase solubility studies*

The phase solubility diagram was established on the basis of the report of Higuchi and Connor's method (Higuchi, 1965). Different concentrations (0, 1, 2, 4, 8, 10% w/v) of aqueous solution of carriers were prepared in different aqueous media containing DDW, pH 7.4, and pH 6.8. Excessive quantity of OND was added to 5 mL of aqueous solution present in each graduated test tube. In a mechanical shaker with constant temperatures at 30, 37, 40 and 45 ± 0.5°C the test tubes were shaken for 24 h. Then the test tubes were centrifuged and the supernatant were filtered through Whatman filter paper (pore size 11 µm) and proper dilutions were made. Later the concentration of OND was determined by UV spectrophotometer at λ<sub>max</sub> 248 nm. In each system the analysis was repeated thrice. Phase-solubility diagram was represented by plotting molar concentration of OND against molar concentration of the carrier. From Eq. (1) apparent stability constants (K<sub>a</sub>) were calculated by using slope and intercept of each profile. Intercept indicates the intrinsic solubility of drug at different temperatures in absence of carrier. The thermodynamic factors were enumerated upon the formation of complex between carrier and drug using Van't Hoff Eq. (Das *et al.*, 2018).

$$K_{1:1} = \frac{\text{Slope}}{\text{Intercept} (1 - \text{Slope})} \quad (1)$$

$$\ln\left(\frac{Ka_2}{Ka_1}\right) = \Delta H \frac{T_2 - T_1}{RT_2T_1} \quad (2)$$

where  $Ka_1$  and  $Ka_2$  are the stability constants at 30 and 37°C and,  $T_1$  and  $T_2$  constitutes the corresponding temperature in Kelvin.  $\Delta H$  denotes Gibbs free energy change and entropy were also determined.  $R$  is the universal gas constant (Das *et al.*, 2018).

#### Preparation of solid dispersion by solvent evaporation method

SDs were composed of different carriers such as HP $\beta$ CD and PVP K-30.OND and carriers taken at suitable ratios (1:1, 1:3 and 1:5 w/w) and produced a dispersion of a physical mixture in an organic solvent mixture (dichloromethane-methanol 1:1 v/v). The solvent was evaporated under vacuum to obtain transparent and solvent-free thin layer. The resultant residue was then dried at 37±0.5°C in a hot air oven until constant weight was achieved (Kahali, Khanam, 2018; Suthar *et al.*, 2013).

#### Aqueous solubility study

Excess amount of SD was taken in 5 mL of DDW, phosphate buffer pH 7.4 and pH 6.8 respectively in graduated stopper test tubes and shaken in a mechanical shaker at 25 and 37°C for 24 h. After that filtration of each sample was done using Whatman filter paper (pore size 11  $\mu$ m). Each filtered solution was then diluted suitably and absorbance was taken at  $\lambda_{max}$  248 nm spectrophotometrically.

#### Measurement of drug content (%) of solid binary system

From each sample of SDs, 10 mg SD were taken and dispersed in 2 mL methanol. Afterwards, each sample was diluted with aqueous media (phosphate buffer pH 7.4) and volume was adjusted to 100 mL in a volumetric flask. Satisfactory dilutions were made further and the content of drug was analyzed in UV spectrophotometer.

#### Characterization of formulations and drug

Pure drug, solid complexes, pure and SD loaded patches were characterized by Fourier Transform Infrared Spectroscopy (FTIR) analysis, study and Scanning Electron Microscopy (SEM).

#### Fourier transform infrared spectroscopic (FTIR) analysis

FTIR analysis was performed to determine the stability of the drug in presence of excipients/polymers and to detect drug-polymer interaction if any. Different samples (OND, SDs, patches) were analyzed using Shimadzu Co., Kyoto; Japan together with Quick Snap sampling modules. The mixture of individual sample and KBr (potassium bromide) was prepared and packed into a disc applying hydraulic pressure. The scanning of sample loaded disc was executed over wavenumber range of 4000-400  $cm^{-1}$  (Kalimuthu and Khanam, 2014).

#### Differential scanning calorimetric study (DSC)

To observe the amorphous and crystalline property of ingredients DSC analysis was carried out. DSC analysis was performed in (Pyris diamond TG/DTA; Perkins Elmer Instruments, Mumbai, India) corroborated with thermal analyser. Approximately 5 mg sample (OND and SDs) was taken in a closed aluminum pan and heated in the range of 20 to 300°C at a heating rate of 10°C/min under a nitrogen flow of 150 mL/min (Das *et al.*, 2018).

#### Scanning electron microscopic analysis (SEM)

In SEM, a tiny electron beam scanned across the surface of the sample molecule to inspect the topographies of samples at very high magnifications. In order to analyse the surface morphology of powder samples and transdermal patches, scanning electron microscopy technique was adopted. The analysis was done using (SEM, JSM-6700F, JEOL Ltd., Japan). The samples were placed individually into the aluminium stub with adhesive tape in both sides. The aluminium

stub is covered with thin layer of platinum under reduced pressure of 2.54 Pa to make it electrically conductive. Through generating 25 mA current under voltage 10 kV the experiment was performed (Kalimuthu and Khanam, 2014).

### Fabrication of transdermal patch

In order to get a homogenized mixture, requisite amount of PVP K30, EC, HPMC and OND (5:1:0.5:1 w/w; 50, 10, 5, 10 mg) were mixed in chloroform and thereafter dibutyl phthalate (30-50% v/w DBP) was added to form transparent and viscous liquid. Another batch of patches

were prepared in the similar way by addition of (30-50% v/w) polyethylene glycol (PEG). The liquid was cast on the backing layer (130 cm<sup>2</sup>, SCOTCHPAK 9733) with the help of an applicator (350 µm, wet film thickness) and dried at 25°C for 24 h. After that an adhesive tape (CoTran™ 9697) was attached to the bottom of the matrix patch. Similarly in respect of SD loaded patches (1:5 w/w OND-PVP K-30 SD, equivalent to 10 mg drug) was taken and the patches were fabricated as mentioned above. Mass balance was confirmed by theoretical amount of drug loaded per square cm of the polymeric film. On the other side, assay method determines the practical amount of drug. In Table I composition of different films is illustrated.

**TABLE I** - Batch of formulations

Patch code	Carriers				Total weight of carriers (mg)	Chloroform (mL)	% DBP (total wt. of polymer)	% PEG (total wt. of polymer)	Drug (mg)
	PVP K30 (mg)	HPMC (mg)	EC (mg)	SD (1:5w/w OND-PVP K-30)					
P1	50	5	10	-	65	3	30% v/w	30% v/w	10
P2	50	5	10	-	65	3	40% v/w	40% v/w	10
P3	50	5	10	-	65	3	50% v/w	50% v/w	10
P4*	-	-	-	78	-	3	30% v/w	30% v/w	10
P5*	-	-	-	78	-	3	40% v/w	40% v/w	10
P6*	-	-	-	78	-	3	50% v/w	50% v/w	10

\* SD was taken as per quantity equivalent to 10 mg OND base for each of the patches, P4-P6.

### Drug Content determination of transdermal patch

1 square cm patch was taken out from each formulation and 2 mL methanol was added and stirred for 1 h. After that volume was adjusted to 100 mL with phosphate buffer pH 7.4 and stirred for 24 h at 60 rpm. The solution was then allowed for sonication for 30 min and filtered through (11 µm pore) Whatman filter paper.

Absorbance was noted after proper dilution at  $\lambda_{max}$  248 nm (Thakur, Singh, Singh, 2016).

### Percentage moisture content

The dried patches were weighed separately and kept in a desiccator consisting of fused calcium chloride for 72 h at 40±0.5°C. After that the patches were reweighed

until constant weight was attained. The difference between initial weight and final weight defined in terms of percentage was used to calculate moisture content (Singh, Bali, 2016).

### **Percentage moisture absorption**

The patches were individually weighed and placed in a desiccator filled with saturated sodium chloride solution with 90% RH for 72 h. The patches were then weighed at random to obtain a constant weight (Thakur *et al.*, 2016).

### **Measurement of thickness of patches**

With the help of digital micrometer screw gauge (Mitutoyo, Japan) the thickness of the dried patches were ascertained at three separate places and the average value was thereafter calculated (Prajapati, Patel, Patel, 2011).

### **Adhesion test (thumb tack test)**

The thumb was put in the sample with slight pressure for a fraction of time and withdrawn instantaneously. It is not difficult to determine how stringent a bond was obtained between skin and adhesive on alteration of pressure and contact time observing the strain to pull out the thumb from adhesive. This thumb tack test, of course, has some loopholes. One is its subjectivity. Another chief loophole is that the data obtained through this test are less quantifiable. Be that as it may, to evaluate adhesiveness of skin bonding it is a method which is undoubtedly most simple. Each sample was tested in three different places for three times (Minghetti, Cilurzo, Montanari, 1999).

### **Tack test by texture Analyzer or Texturometer**

The Texture analyzer or texturometer (Texture Technologies Corp, Marietta, GA, USA) comprises 7 mm probe which is employed to ascertain the adhesion capacity of pure and SD loaded patches (Zheng, Reza, 2014; Elsabee, Abdou, 2013; Puri *et al.*, 2019). The patches were prepared with two different plasticizers, PEG and DBP and stored for one month at room temperature ( $25\pm 1^\circ\text{C}$ ). Before performing the test samples, the

analyzer was calibrated and different parameters like: target force, approach and return speed, distance as well as hold time were reformed. From each sample  $3.0\text{ cm} \times 3.0\text{ cm}$  patch was cut and fixed on the sample holding unit without addition of release liner. The probe was allowed to come into the contact with adhesive patches with a target force (50 g) and holding time (10 sec) as the test runs were initiated. This process produced a bond between the surface of the probe and patches. Afterwards, the probe was pulled off and it causes debonding between two surfaces. Finally, the parameters such as: work of adhesion, positive area and separation distance were detected.

### **In-vitro diffusion study**

*In-vitro* release studies were performed in Franz diffusion cells which has two distinct sections- donor cell and receptor cell. The donor cell is a long cylindrical tube both ends of which are open and the lower portion is such as can be flexibly adjusted with the neck of receptor cell. The total volume of receptor part is 50 mL and it is equipped with an external jacket which functions as a tool to maintain the temperature at  $37\pm 0.5^\circ\text{C}$ . The receptor cell was affixed on the multicell magnetic stirrer. It was then filled with phosphate buffer pH 7.4 (50 mL). At the lowest part of the donor cell release liner with drug loaded patch ( $3.935\text{ cm}^2$  circular area) was fixed. From the receptor cell samples were taken out at definite time intervals and equal volume of same buffer was replaced during the experiment. The concentration of drug present in each sample was measured by UV spectrophotometer at wavelength of 248 nm. Amount of drug diffused was calculated and cumulative percent release (CPR) was resolved to enumerate the amount met with each sample

### **Ex-vivo permeation study**

*Ex-vivo* permeation study was performed by using excised porcine ear portion with an area of  $3.935\text{ cm}^2$ . Porcine skin has been chosen to perform the ex-vivo permeation study because it is anatomically similar with human skin as well as it is widely available in the market

(Schmook, Meingassner, Billich, 2001). With treatment of phosphate buffer pH 7.4 for 2 h external debris was removed and equal area of skin of donor compartment was cut and attached between donor and receptor portion (Das, Ghosal, 2008). The receptor part contains pH 7.4 buffered media. Before permeation study of formulations it is necessary to ascertain whether any impurities/skin components are present in receptor media. To analyze the skin impurities dermal side of the skin (without formulation) was kept in contact of receptor media and a fixed volume of sample (5 mL) was withdrawn at a regular time interval and same volume of freshly prepared pH 7.4 buffer was replaced after each withdrawal and analyzed spectrophotometrically (Kaur, Geetha, Kakkar, 2011). For permeation of formulations, pure drug and SD loaded patches was attached each in the donor cell which is in contact with the stratum corneum (SC) part of ear skin. Samples were withdrawn and cumulative amount of drug which permeates through the skin was observed under UV-spectrophotometer at 248 nm.

In this context it is noted that at the time of diffusion and permeation the solubility data in different aqueous media were considered for the purpose of maintaining sink condition and, therefore, appropriate quantity of drug is loaded in the donor compartment of the diffusion cell.

### **Drug Content uniformity**

To determine the drug content uniformity the patches were stored in a desiccator for 6 months and analyzed the influence of variability of drug content on films stability. In a 100 mL volumetric flask SD loaded patches (1 cm<sup>2</sup> each) were taken and 2 mL methanol was added in it. The mixed content was then stirred for 2 h for extraction of drug. Extraction of drug having been done the remaining volume was adjusted to 100 mL with pH 7.4 phosphate buffered media and thereafter sonicated for 4 h. The samples were then filtered. After preparation of proper dilutions the samples were measured with the help of UV-spectrophotometer (Banerjee *et al.*, 2014).

### **Statistical analysis**

The data as assessed were described as mean±standard deviation (S.D) and measurement in each case was done three times. The difference that present between the sets was tested by students' t-test at the standard  $p < 0.05$  wherever necessary.

## **RESULTS AND DISCUSSION**

### **Study of saturation solubility**

The study of saturation solubility was performed in an aqueous media of DDW (~pH 6.0), pH 7.4 and pH 6.8 respectively. It is evident that OND is a weakly basic drug ( $pK_a=7.4$ ) and under acidic pH it is aqueous soluble (Salem, Lopez, Galan, 2001). Hence the drug remains unionized at pH 7.4 which is considered as in-vitro study fluid in the present work. Notably, the influence of acidic pH on solubility was also to be observed. In each aqueous media (DDW, pH 7.4, pH 6.8) the concentration of OND was found to be  $187 \pm 0.007$ ,  $188.48 \pm 0.007$ ,  $451.23 \pm 0.006$   $\mu\text{g/mL}$  and  $253.10 \pm 0.004$ ,  $216.36 \pm 0.002$ ,  $512.96 \pm 0.004$   $\mu\text{g/mL}$  respectively at 25° and 37°C. These values reveal that in basic media the solubility is apparently decreased as compared to acidic media.

### **Partition coefficient**

In octanol-water ( $K_o/w$ ) and octanol-phosphate buffer pH 7.4 the partition coefficient of OND HCl, OND and its SDs were found ( $\text{Log } P = 2.43 \pm 0.005 - 2.85 \pm 0.01$ , Table II). From the results of partition coefficient, it was confirmed that Log P values of OND and all the formulations agree to the reported value. The Log P values obtained in case of OND and other formulations were higher than that of hydrochloride form. It stipulates that OND and SDs have higher lipophilicity than the former one. Thus, modification of drug and its SDs have more favorable impact on skin permeation.

**TABLE II** - Study of Partition coefficient

Formulations	Log P value in octanol-water	Log P value in octanol-pH 7.4 buffer
OND HCl	2.43±0.002	2.36±0.003
OND	2.52±0.005	2.45±0.01
*OND: HPβCD(1:1 w/w)	2.58±0.01	2.49±0.001
*OND: HPβCD(1:3 w/w)	2.64±0.002	2.54±0.004
*OND: HPβCD(1:5 w/w)	2.73±0.005	2.59±0.005
*OND: PVP K-30 (1:1 w/w)	2.52±0.004	2.60±0.002
*OND: PVP K-30(1:3 w/w)	2.61±0.002	2.66±0.001
*OND: PVP K-30(1:5 w/w)	2.85±0.01	2.78±0.001

\*SDs

### Phase solubility study

Phase solubility profile of OND-HPβCD and OND-PVP K-30 was established by plotting concentration of OND (Mole/L) against concentration of carrier (Mole/L). From each profile slope and intercept were calculated to determine the stability constant ( $K_a$ ) and other thermodynamic parameters such as change in free energy ( $\Delta G$ ), change in enthalpy ( $\Delta H$ ) and change in entropy ( $\Delta S$ ) of the system. These complexes satisfactorily modify the

features of solubility of drug. In order to measure the effects of complexation ability of two carrier systems phase solubility study of binary system was carried out. At different temperatures (303 K, 310 K, 313 K and 318 K) the pattern of isotherms of phase solubility profiles are AL type for both the cases of HPβCD and PVP K-30 system (Figure 1). AL type linear isotherms explain the enhancement of solubility of a guest mole as a function of concentration of carrier.

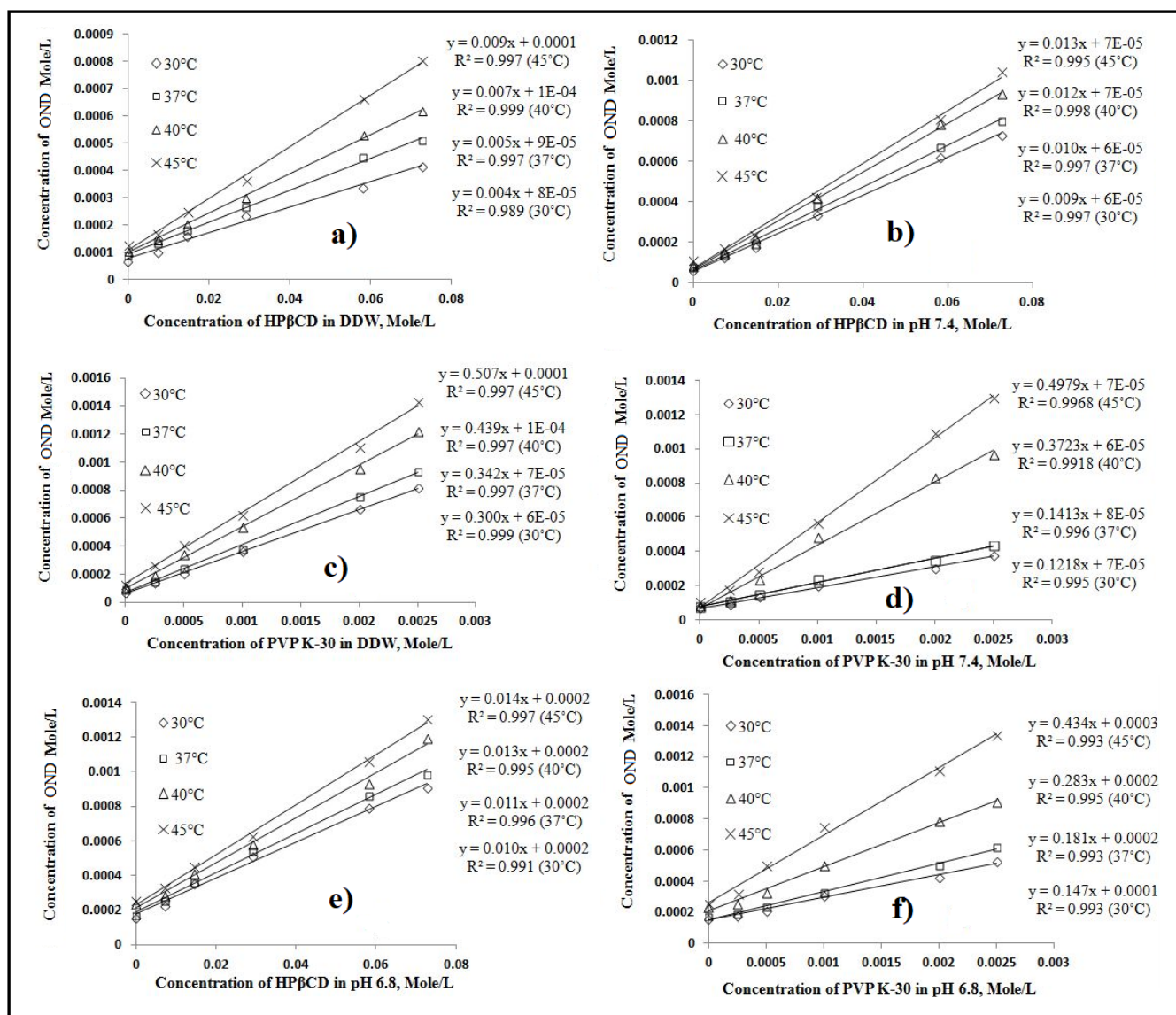


**FIGURE 1** - Phase solubility analysis of a) HPβCD-OND at DDW; b) HPβCD-OND at pH 7.4; c) PVP K-30-OND at DDW; d) PVP K-30-OND at pH 7.4; e) HPβCD-OND at pH 6.8; f) HPβCD-OND at pH 6.8 at different temperatures.

The binary systems showed the negative free energy change which indicates spontaneous solubilization. Free energy change ( $\Delta G$ ) varies from -17.76 to -24.8 kJ/mol and -10 to -13 kJ/mol for PVP K-30 and HPβCD respectively. It implies that the molecules of drug may bind with the weak physical forces like Vander Waals' force, hydrogen bonding and hydrophobic forces. Effects of temperature on  $K_a$  in all cases were much prominent. Binding constants of PVP K30-OND and HPβCD-OND binary systems were decreased in the order of DDW>pH 7.4>pH 6.8 and pH 7.4>DDW>pH 6.8. Degree of dissociation of OND

enhances with decrease in pH. This feature may not suit hydrophobic binding. So, stability constant value ( $K_a$ ) decreases in acidic pH. This is because of less interaction between ligand and guest molecules.

The change in stability constant was possibly due to dipole-dipole induced complexation of amide group of PVP K-30 with OND and also due to hydrogen bonding between the carbonyl group of PVP K-30 as well as hydrogen atom in the carbonyl (C=O) group of OND. The hydrogen atoms in the PVP K-30 and OND squeeze out surrounding water molecules. Due to this binding, water molecules become

less ordered and yield enhanced entropy (+ $\Delta S$ ) upon complexation in most of the cases. As a matter of fact PVP K-30 has its hydrophobic and hydrophilic parts which may be considered as the respective sites for its adherence with drug molecules (for both undissociated and dissociated). Endothermic ( $\Delta H$ ) type of complexation was found in this study. Further, entropy change ( $\Delta S$ ) was found positive except in case of HP $\beta$ CD at 37°C. This may be due to higher flexibility of broader ring of HP $\beta$ CD. Moreover, cyclodextrins belong to the class of oligosaccharides containing ( $\alpha$ -1,4)-linked  $\alpha$ -D-glucopyranose units along with hydrophilic outer and lipophilic inner surfaces. Thus, cyclodextrins can form water soluble amorphous inert inclusion complexes with number of poor water soluble candidates (Das *et al.*, 2018, Di, Kerns, 2016).

Free energy change ( $\Delta G$ ) was found negative in all cases. Negative  $\Delta G$  ensures spontaneous complex formation. Highly negative  $\Delta G$  values and positive entropy suggest that complexation was favored in higher pH in comparison to lower pH. Higher  $K_a$  value of PVP K-30-OND binary system (7160.9-7913.6 M<sup>-1</sup>, 25-45°C) indicates increase in solubility than that of HP $\beta$ CD-OND binary system (54.43-86.91 M<sup>-1</sup>, 25-45°C) in different aqueous media. Sometimes it was noticed that if stability constant is too high, it may form a more stable complex. So, drug may not be released out to a greater extent from the complexed state (Kalimuthu, Khanam, 2014). Solubilization depends on pH of medium due to degree of ionization. The data of phase solubility study is illustrated in Table. III.

**TABLE III** - Thermodynamic parameters for the reciprocation of Ondansetron with PVP K30 and HP $\beta$ CD

Carrier	Temperature in °C	Temperature in K	DDW (kJ/Mole)		pH 7.4 (kJ/Mole)		pH 6.8 (kJ/Mole)	
			* $K_a$ , M <sup>-1</sup>	(* $\Delta G$ , * $\Delta H$ , * $\Delta S$ )	$K_a$ , M <sup>-1</sup>	( $\Delta G$ , $\Delta H$ , $\Delta S$ )	$K_a$ , M <sup>-1</sup>	( $\Delta G$ , $\Delta H$ , $\Delta S$ )
PVP K30	25	303	7160.9	$\Delta G = -22.36$ $\Delta H = 4.42$ $\Delta S = 0.088$	3157.16	$\Delta G = -20.29$ $\Delta H = 60.82$ $\Delta S = 0.267$	1156.77	$\Delta G = -17.76$ $\Delta H = 27.37$ $\Delta S = 0.148$
	37	310	7450.53	$\Delta G = -22.97$ $\Delta H = 13.32$ $\Delta S = 0.11$	5446.01	$\Delta G = -22.17$ $\Delta H = 79.14$ $\Delta S = 0.326$	1478.41	$\Delta G = -18.81$ $\Delta H = 65.52$ $\Delta S = 0.272$
	40	313	7829.13	$\Delta G = -23.33$ $\Delta H = 1.77$ $\Delta S = 0.08$	7309.83	$\Delta G = -23.15$ $\Delta H = 84.82$ $\Delta S = 0.344$	1886.39	$\Delta G = -19.62$ $\Delta H = 74.02$ $\Delta S = 0.299$
	45	318	7913.6	$\Delta G = -23.73$	12203.6	$\Delta G = -24.87$	2950.37	$\Delta G = -21.12$
HP $\beta$ CD	25	303	54.43	$\Delta G = -10.06$ $\Delta H = 20.62$ $\Delta S = 0.10$	158.66	$\Delta G = -12.76$ $\Delta H = 10.05$ $\Delta S = 0.075$	58.21	$\Delta G = -10.23$ $\Delta H = 3.95$ $\Delta S = 0.046$
	37	310	65.49	$\Delta G = -10.77$ $\Delta H = 19.77$ $\Delta S = 0.098$	173.62	$\Delta G = -13.29$ $\Delta H = 12.39$ $\Delta S = 0.082$	60.31	$\Delta G = -10.56$ $\Delta H = 4.60$ $\Delta S = -0.008$
	40	313	70.49	$\Delta G = -11.07$ $\Delta H = 34.65$ $\Delta S = 0.146$	181.81	$\Delta G = -13.53$ $\Delta H = 5.16$ $\Delta S = 0.059$	61.35	$\Delta G = -10.71$ $\Delta H = 6.09$ $\Delta S = 0.053$
	45	318	86.91	$\Delta G = -11.80$	187.57	$\Delta G = -13.83$	63.65	$\Delta G = -10.98$

\* $K_a$  = binding constant, \*  $\Delta G$  = change in Gibbs-free energy, \* $\Delta H$  = change in enthalpy, \* $\Delta S$  = change in entropy

### Aqueous solubility study and drug content determination

OND is poorly soluble in double distilled water ( $\sim 187 \pm 0.007 \mu\text{g/mL}$ ,  $25^\circ\text{C}$  and  $253.10 \pm 0.004$ ,  $37^\circ\text{C}$ ). Solubility of OND increases linearly when fraction of PVP K-30 in SD is increased. Solubility was enhanced upto the drug-carrier ratio 5:1 (w/w) as drug amount was fixed (100 mg). Solubility of drug in case of all binary mixtures of PVP K-30-OND was obtained higher than that of HP $\beta$ CD-OND binary system at both 25 and  $37^\circ\text{C}$ . Enhancement of solubility was found 4.0-4.5 times higher as compared to pure drug in pH 7.4. Besides, in DDW ( $\sim \text{pH } 6$ ) the solubility was found  $\sim 4.75$  times. This may be due to high

solubility of OND in lower pH. As the enhanced solubility favours ionization, the phenomenon of enhancement of solubility confirmed that in lower pH the drug (OND) has been ionized. Enhancement of solubility was found low ( $\sim 1.8$ - $2.11$ ) times in case of pH 6.8 as compared to pure drug. Enhancement of solubility for all binary systems was expressed as  $(1:5 > 1:3 > 1:1)$ , Figure 2). As the lipophilicity of drug and other SDs do increase ( $2.45 \pm 0.01$ - $2.78 \pm 0.001$ , pKa), so does increase the solubility. SD refers to a group of solid products containing two different elements, generally a hydrophilic matrix and a hydrophobic drug. For the binary system, the hydrophilic properties of PVP-K30 increased the solubility according to increase in temperature than HP $\beta$ CD, although the difference was not much wide.

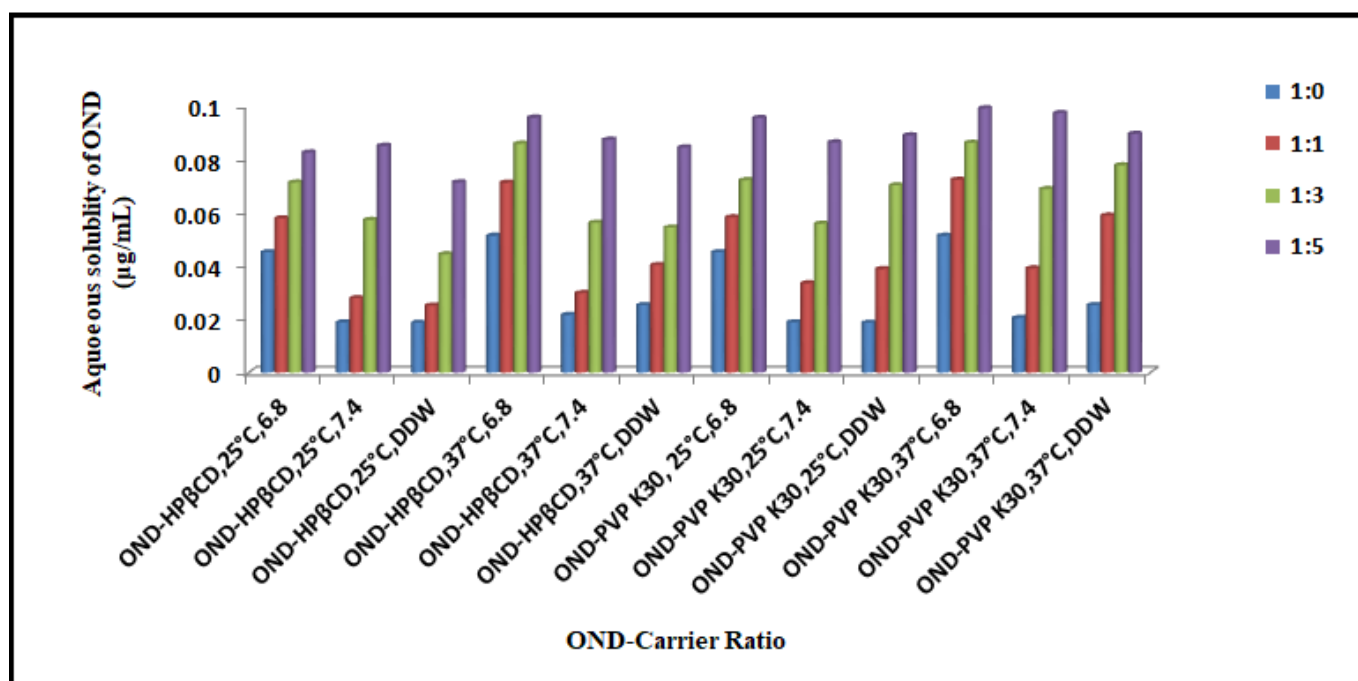


FIGURE 2 - Aqueous solubility of OND in different pH at 25 and  $37^\circ\text{C}$ .

The drug content of each binary system (1:1, 1:3 and 1:5 w/w) was found  $4845 \pm 3$ ,  $2412.72 \pm 3.4$ ,  $1520 \pm 8.7 \mu\text{g/mL}$  and  $4772.72 \pm 4.5$ ,  $2472 \pm 1.1$ ,  $1527 \pm 8.3 \mu\text{g/mL}$  respectively for HP $\beta$ CD and PVP K-30. The data of solubility study of each system were depicted in Table IV.

**TABLE IV** - Solubility study of OND and OND-SD

Carrier-Drug Ratio (w/w)	Temperature (°C)	Solubility in DDW ( $\mu\text{g/mL}$ )	Solubility at pH 6.8 ( $\mu\text{g/mL}$ )	Solubility at pH 7.4 ( $\mu\text{g/mL}$ )
PURE OND	25	187 $\pm$ 0.03	451.23 $\pm$ 0.03	188.48 $\pm$ 0.02
	37	253.10 $\pm$ 0.0	512.96 $\pm$ 0.04	216.36 $\pm$ 0.02
OND:HP $\beta$ CD (1:1 w/w)	25	251.41 $\pm$ 0.02	578.39 $\pm$ 0.01	285.45 $\pm$ 0.005
	37	403.38 $\pm$ 0.004	711.72 $\pm$ 0.04	298.18 $\pm$ 0.04
OND:HP $\beta$ CD (1:3 w/w)	25	443.50 $\pm$ 0.02	712.34 $\pm$ 0.02	578.18 $\pm$ 0.05
	37	543.50 $\pm$ 0.06	858.02 $\pm$ 0.002	561.81 $\pm$ 0.03
OND:HP $\beta$ CD (1:5 w/w)	25	712.99 $\pm$ 0.03	824.69 $\pm$ 0.006	850.30 $\pm$ 0.01
	37	844.06 $\pm$ 0.01	956.17 $\pm$ 0.03	872.72 $\pm$ 0.06
OND:PVP K-30 (1:1 w/w)	25	388.13 $\pm$ 0.05	582.09 $\pm$ 0.004	334.54 $\pm$ 0.008
	37	588.70 $\pm$ 0.01	722.83 $\pm$ 0.006	390.90 $\pm$ 0.002
OND:PVP K-30 (1:3 w/w)	25	702.25 $\pm$ 0.01	720.98 $\pm$ 0.004	558.18 $\pm$ 0.02
	37	776.83 $\pm$ 0.06	861.11 $\pm$ 0.03	687.87 $\pm$ 0.001
OND:PVP K-30 (1:5 w/w)	25	889.26 $\pm$ 0.04	954.93 $\pm$ 0.01	863.03 $\pm$ 0.002
	37	894.91 $\pm$ 0.009	990.74 $\pm$ 0.01	972.72 $\pm$ 0.003

### Carrier, plasticizer and solvent selection for preparation of current transdermal device

When hydrophilic compound- PVP K-30 is added to EC which is a hydrophobic film forming polymer, enhancement of release rate constants happens to occur. This effect can be ascribed to leaching of soluble component which helps to form pores and yields a reduction in mean diffusion path length of drug molecules to be released into diffusion medium. Moreover PVP K-30 acts as an anti-nucleating agent that restrains the crystallization of drug (Kandavilli, Nair, Panchagnula, 2002).

In controlled drug delivery system HPMC is used rapidly. It is a hydrophilic swellable polymer having film forming property. HPMC is adequately soluble in aqueous media and hence it produces transparent film (Rogers, 2009, Kandavilli *et al.*, 2002).

Plasticizer has an outstanding role in the development of transdermal patches. It confers flexibility as well as

mechanical strength and adhesive property to the polymeric matrix. Generally, low molecular weight is the prime factor for the selection of plasticizer because it minimizes secondary bonds amongst polymer chains in matrix (Gal, Nussinovitch, 2009). In this context, the effect of low molecular weight hydrophobic plasticizer (DBP, 278.35 g/mol) was chosen. Whereas, and high molecular weight hydrophilic plasticizer (PEG, 4500 g/mol) was selected for the preparation of patches because it is non-toxic, highly miscible and biodegradable in nature. Both DBP and PEG (30-50% v/w) is added to prepare patches to compare the effects on permeation flux as well as release.

The relative polarity and dielectric constant of chloroform are 0.259 and 4.81 respectively. On the basis of these characters, chloroform was selected as casting solvent for the development of transdermal film. From the aforementioned values it is clear that chloroform is an apolar solvent, in which when drug is administered, minimizes the crystallinity of drug (Pattnaik *et al.*, 2011).

### Percentage moisture content, moisture absorption and drug content studies

The stability of ideal patches was described by lower percentage of moisture content (MC). Presence of less moisture content yields dried patches which are very essential characteristic for transdermal devices. Lower moisture absorption (MA) confirms inhibition of growth of microorganisms and thereby minimizes less toxicity

and irritation to skin. Approximately 87-96.9% drug content (DC) was found in each patch ensures almost equal distribution of drug. Lower percentage uptake as well as less moisture content was observed in case of DBP containing patches as compared to PEG. This may be due to hygroscopic nature of PEG which causes higher moisture absorption in patches. All the results were found statistically significant ( $p < 0.05$ ). Table V illustrates the values of %MC, % MA and %DC.

**TABLE V** - Data of Percentage moisture content, percentage moisture absorption and percentage drug content. ( $n=3$ )

Patch code	% MC		% MA		% DC	
	PEG	DBP	PEG	DBP	PEG	DBP
P1	1.29±0.06	1.11±0.032	3.14±0.2	1.28±0.71	91.39±1.04	94.53±0.02
P2	1.28±0.045	1.21±0.051	3.37±0.31	1.92±0.32	92.18±1.81	96.91±2.36
P3	1.31±0.02	1.06±0.035	1.97±0.15	1.01±0.2	87.45±1.81	93.76±4.92
P4*	2.77±0.047	1.89±0.043	3.64±0.04	1.90±0.023	92.18±3.14	96.12±2.09
P5*	3.10±0.023	2.22±0.031	3.83±0.052	2.62±0.02	94.54±1.81	95.33±1.04
P6*	2.41±0.04	1.23±0.012	2.79±0.046	2.10±0.031	92.18±3.63	95.33±3.78

### Thickness, adhesion property and content uniformity

On experiment the thickness of transdermal patches appeared to be satisfactory, and the thickness as measured was 0.084±0.006 to 0.089±0.008 mm ( $p < 0.05$ ). As the thickness of patches increases, the tightness of molecules also increases. This phenomenon lowers down the mobility of molecules. As a result drug release from patches functions in a very controlled manner.

It is to be noted that in all cases of formulations except P3 and P6 with PEG the result of adhesion property causes better adhesive character. The presence of PVP K-30 to a greater amount ultimately makes the adhesion property better because PVP K-30 itself acts as an adhesive in patches (Kathe, Kathpalia, 2017). When mixed with DBP, minimizes hardness of patches.

It was found that higher volume of DBP boosts up the flexibility and increases adhesive property to a greater extent.

The content uniformity was found optimized in case of pure drug loaded patches (P1-P3) as well as (1:5 w/w OND-PVP SD, P6\*) loaded patches (86.67±2.7-95.33±2.7%,  $p < 0.05$ ). In doing so, no illustrious differences could be observed between pure drug and SD patches. With slight standard deviation values of every drug contents were found more or less the same. This result clearly reveals the fact that drug was well distributed throughout the patches. Temperature or relative humidity could not create any collision in drug content uniformity in this case.

The values of thickness, adhesion character and content uniformity of films are reported in Table VI.

**TABLE VI** - Thickness, adhesion property and content uniformity of different patches ( $n=3$ )

Patch code	Thickness (mm)		Adhesion property		Drug content uniformity (%)	
	PEG	DBP	PEG	DBP	PEG	DBP
P1	0.086±0.009	0.084±0.006	+++	+++	89.03±2.7	91.38±5.9
P2	0.089±0.004	0.086±0.0025	+++	+++	90.60±3.7	94.54±2.36
P3	0.089±0.003	0.084±0.005	+	++	86.67±2.7	92.18±2.36
P4*	0.086±0.002	0.089±0.008	+++	+++	88.24±4.5	95.33±2.7
P5*	0.085±0.004	0.088±0.003	+++	+++	91.39±3.78	93.76±3.78
P6*	0.085±0.004	0.089±0.003	+	+++	89.03±2.0	92.97±2.7

+++Excellent adhesion property, ++good adhesion, +poor adhesion property

### Tack properties by Texturometer or Texture analyzer

The adhesiveness of transdermal patch is analysed by testing its tack, which is a calculated force of debonding upon the utilization of small pressure for a short period of time. In this study the application of probe tack test was done. The force is necessary to separate the probe from the adhesive surface of a transdermal patch was measured. The highest value of force that is needed

to break the bond between the probe and patches after longer period of contact is expressed as tack (Cilurzo, Gennari, Minghetti, 2012). The adhesive properties (absolute positive force), work of adhesion as well as average separation distance of patches (P1-P6\*) were measured thrice after storage of one month. DBP loaded SD patches (P4\*-P6\*) Good adhesive nature was found in the cases of DBP-SD patches as compared to pure drug (P1-P3) and PEG-SD patches (P4\*-P6\*). The result of each formulation (P1-P6\*) are illustrated in Table VII.

**TABLE VII** - Tack properties of different patches ( $n=3$ )

Patch code	Adhesive properties (g/cm <sup>2</sup> )		Work of adhesion (g.s)		Average separation distance (mm)	
	PEG	DBP	PEG	DBP	PEG	DBP
P1	1216.76±149.54	1104±176.49	32.49±9.12	33.89±10.30	1.33±0.52	1.26±0.5
P2	1019.12±124.78	1156±216.06	35.72±7.39	36.46±9.16	1.20±0.70	1.34±0.63
P3	1072.84±163.46	1095.40±115.94	27.39±7.11	38.73±10.59	1.67±0.27	1.38±0.6
P4*	1227.38±182.60	1279±208.77	39.24±10.21	33.23±8.66	1.34±0.5	1.10±0.12
P5*	1165.89±204.19	1180±136.72	34.12±9.48	35.69±8.45	1.29±0.5	1.22±0.18
P6*	1110.34±146.44	1294.85±221.09	39.52±10.31	40.91±9.88	1.23±0.35	1.18±0.21

### In-vitro diffusion study

In-vitro diffusion analysis (Figure 3) was performed an in-vitro version of Keshary-chien cells. Before the analysis of patches it is essential to check the drug release behavior. To check the same, a similar amount (302.69 µg) of OND as present in 3.935 cm<sup>2</sup> patch has been taken in

donor cell (previously covered with cellophane membrane and release liner) as a solution form (3 mL OND solution made up with chloroform) in phosphate buffer pH 7.4 and 36.07±0.31% drug was diffused after 8 h. This indicates that OND controls the release mechanism more efficiently as it showed retarding effect. The study of in-vitro diffusion of patches was carried out at 37±0.5°C.

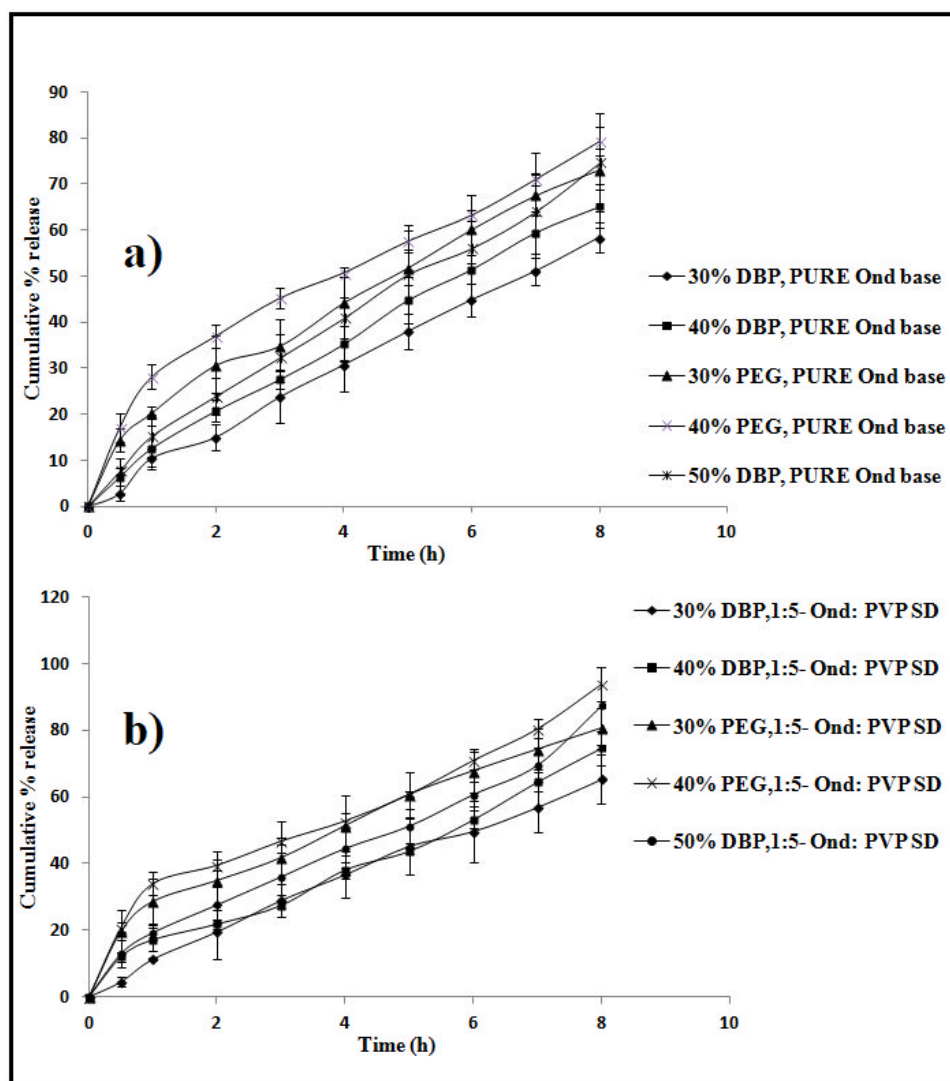


FIGURE 3 - In-vitro diffusion profile of a) Pure OND loaded patches b) SD loaded patches.

Increase of percentage of plasticizer shows increased drug release from the patches. Drug release is observed higher in cases of SD loaded patches as compared to pure drug loaded patches. It was also observed that the patches with PEG showed higher drug release than that

of DBP loaded patches. This is because of hydrophilic nature of PEG which in combination with higher fraction of hydrophilic carriers such as: PVP K-30 and HPMC causes increased drug release from the patches. Apart from that, a significant effect of EC was observed in case

of drug release. EC formed pores with swellable polymer HPMC which leads rapid diffusion of drug through the membrane to the medium (Patel *et al.*, 2009).

After 8 h the cumulative percentage release for 30%, 40%, 50% v/w DBP (P1-P3) and 30%, 40% v/w PEG (P1 and P2) loaded patches for pure drug were obtained 58.41±3.22, 65.10±4.74, 74.65±10.58% and 73.21±4.55, 79.25±3.16% drug release respectively. Conversely, enhanced drug release was observed in all cases of SDs loaded patches as compared to pure drug. Enhancement of concentration of plasticizer facilitates the release of drug and the drug release also consequently increases. Flexibilities of carrier macromolecular segments are increased by plasticizer of higher percentage. Loosening of tightness of intermolecular forces thus happens to occur (Bergo, Sobral, 2006). With increase of volume of plasticizer the flow property of drug molecules increases relatively. Hence, better release is attained. The cumulative percentage drug release of SD-PEG (30-40% v/w i.e. P4\* and P5\*) and SD-DBP (30-50% v/w i.e. P4\*-P6\*) patches were found 80.59±6.11, 93.79±7.81% and 65.30±7.45, 74.58±5.23, 87±11.65% respectively after 8 h.

It is to be noted that as the patches (P3 and P6\*) with 50% PEG showed poor adhesion property and appeared less smooth in nature, further experiments were not done for those patches.

### Ex-vivo skin permeation study

After 8 h of constant evaluation very small amount of skin component was observed. This happens possibly because of presence of little quantity of aqueous soluble UV absorbing substance which comes out through skin. Before the evaluation of drug-carrier loaded patches, it is necessary to observe whether the plain drug can permeate through the skin or not. So as to evaluate drug-carrier loaded patches, first of all, what is necessary is to analyse if the pure drug can permeate through skin or not. Therefore, the experiment was performed at 37±0.5°C by fastening the skin (3.935 cm<sup>2</sup>) onto the donor cell and a solution (302.69 µg in 3 mL chloroform) of plain drug was put upon the slice of the skin affixed on the donor cell. The top most opening of the donor compartment

is closed with parafilm. About 28.44±0.052% (Data not mentioned) drug was permeated across the skin with flux of 0.80±0.14 µg/cm<sup>2</sup>/h.

In *ex-vivo* experiment of formulations, it was noticed that P4\* and P5\* with PEG showed permeation (215.93±7.51, 255.36±4.64 µg) higher than that of P1 and P2 (186.27±5.04 and 218.51±5.85 µg) through 3.935 cm<sup>2</sup> barrier after 8 h. Whereas DBP-SD (P4\*-P6\*) and DBP-pure drug loaded patches (P1-P3) showed less amount of drug permeation (P1= 156.30±21.81, P2=177.18±12.84, P3=204.33±11.67; P4\*=176.24±9.24, P5\*=206.06±10.81, P6\*=236.48±3.66 µg/3.935 cm<sup>2</sup>) after 8 h as compared to patches with PEG. The reason behind this is possibly leaching out of fraction of PEG from the patches which form smaller pores. Thus, higher permeability is occurred. The reason behind occurrence of higher permeability in respect of patches with SD is the presence of higher fraction of PVP K-30 which helps augmentation in solubility and thermodynamic issues in the media that gives rise to enhanced permeability of the drug.

Table VIII illustrates the parameters of permeation and the plots are represented in (Figure 4a-b). The augmentation of flux (JSS) was observed higher in SD loaded patches having higher fraction of plasticizers. The highest enhancement of permeability flux (8.42 fold) was observed in case of P5\* (40% PEG-SD) patch. This is because of a good miscible property of PEG with PVP K-30 and also due to presence of higher amount of PVP K-30 which diffuses well in PEG network. Plasticizing effect is an important parameter for working on films with SDs. Among all the DBP-SD loaded patches, P6\* brings forth the highest flux because of presence of higher percentage of plasticizer. The improvement of solubility is due to low molecular weight of DBP. Low molecular weight plasticizer enhances pliability and thereby decreases the glass transition temperature of polymer. However, it was previously observed that the films plasticized with PEG gained higher moisture content. The similar effect was observed by (Rao, Diwan 1997). Thus, from all the formulations 50% v/w DBP-SD (1:5 OND-PVP K-30) loaded patch found optimized and the flux as obtained does not differ much from 40% v/w PEG-SD (1:5 OND-PVP K-30) loaded patch.

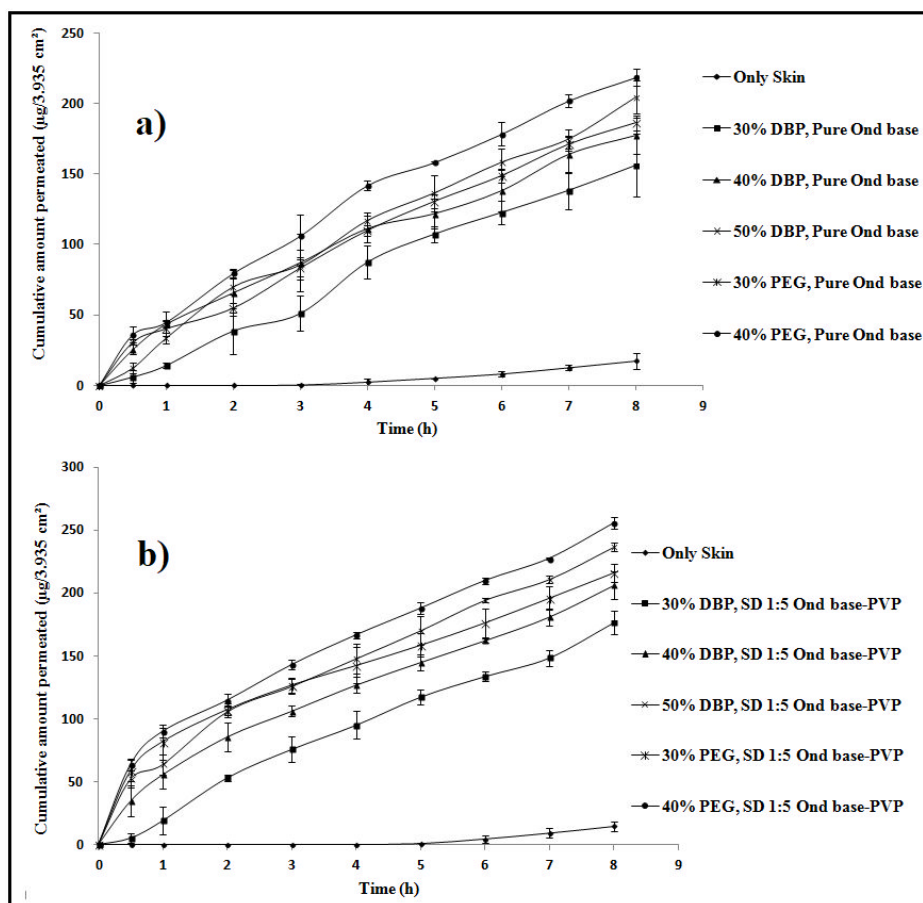


FIGURE 4 - Ex-vivo permeation profile of a) Pure drug loaded patch b) SD loaded patches.

TABLE VIII - Permeation parameters of different formulations (n=3)

Formulation code	R <sup>2</sup> value		Flux, J <sub>ss</sub> (µg/cm <sup>2</sup> /h)		K <sub>p</sub> (cm/h)		Enhancement factor of flux (J <sub>ss</sub> )	
	PEG	DBP	PEG	DBP	PEG	DBP	PEG	DBP
PURE OND	0.984		0.80±0.14		0.24±0.2		-	
P1	0.987±0.004	0.979±0.006	5.02±0.59	5.48±0.48	0.164±0.02	1.47±1.22	6.27	6.85
P2	0.975±0.01	0.963±0.01	5.51±1.87	5.57±0.057	0.151±0.04	0.221±0.025	6.88	6.96
P3	-	0.985±0.004	-	6.23±0.59	-	0.541±0.17	-	7.78
P4*	0.921±0.02	0.982±0.007	5.63±0.77	5.68±0.45	0.097±0.02	1.64±1.20	7.03	7.10
P5*	0.942±0.006	0.958±0.01	6.74±0.23	6.44±0.22	0.106±0.011	0.20±0.06	8.42	8.05
P6*	-	0.959±0.01	-	6.64±0.18	-	0.12±0.02	-	8.30

R<sup>2</sup>= Rrgression coefficient according to zero order kinetics, K<sub>p</sub>= permeation coefficient

The release profiles were prone to zero-order, first-order and Higuchi model (Table IX). The in-vitro release profiles did not ratify to zero-order kinetics. Among all the formulations, the formulations prepared with pure OND (P1-P3) follows first order kinetics except 50% DBP loaded patch (P3). Molecules diffused from multi-polymeric matrix device, often depends upon structural characteristics of polymeric blend. Diffusion in polymers takes place across the amorphous matrix system and the diffusivity of drug molecule is associated with the movement of polymer chain and thereupon to the free volume of the system. The rate and extent of drug molecules released from the matrix with respect

to time is proportional to the diffusional path length and thereupon the volume of the device. Hence, the formulations followed first order kinetics.

Whereas, the formulations with SD (P4\*-P6\*) and P3 (50% DBP loaded patch) follows Higuchi model. This is because the resulting concentration of drug in the media is much lower as compared to saturation solubility of drug molecule in *in-vitro* fluid media and resultantly the sink condition is maintained. On the contrary, the presence of EC in matrix inhibits the swelling of hydrophilic polymers when comes to the contact of aqueous fluid media (pH 7.4) and hence the constant diffusivity of drug is occurred.

**TABLE IX** - Kinetic study of pure OND and SD loaded patches

Patch code	Models	Coefficient of determination (R <sup>2</sup> )		Release Mechanism	
		DBP	PEG	DBP	PEG
P1	Higuchi	0.976	0.973		
	Zero order	0.991	0.989	First order	First order
	First order	0.993	0.990		
P2	Higuchi	0.988	0.989		
	Zero order	0.980	0.980	First order	First order
	First order	0.991	0.992		
P3	Higuchi	0.990	-		
	Zero order	0.989	-	Higuchi	-
	First order	0.984	-		
P4*	Higuchi	0.991	0.990		
	Zero order	0.990	0.925	Higuchi	Higuchi
	First order	0.990	0.983		
P5*	Higuchi	0.992	0.991		
	Zero order	0.970	0.944	Higuchi	Higuchi
	First order	0.985	0.956		
P6*	Higuchi	0.990	-		
	Zero order	0.962	-	Higuchi	-
	First order	0.976	-		

## Characterization of formulations

### FTIR spectroscopic analysis

The solid-state interaction between carrier and drug is described by FTIR spectroscopy. FTIR spectra of OND HCl, OND, carriers (HP $\beta$ CD, PVP K-30), SDs and patches were characterized by FTIR analysis. At 3412 to 3245.31  $\text{cm}^{-1}$ , FTIR spectra of OND HCl (Figure 5.1 a) showed sharp peak for -OH band stretching. At 1639.49  $\text{cm}^{-1}$  and 2976.16  $\text{cm}^{-1}$  C=O and C-H stretching were observed (Patil *et al.*, 2015). In case of OND the spectra (Figure 5.1 b) showed a prominent peak at 1622.13  $\text{cm}^{-1}$  which indicates presence of C=O group. The C-H stretching was observed at 2935.66 to 2987.74  $\text{cm}^{-1}$ . The peaks present at 1639.49  $\text{cm}^{-1}$  and 2976.16  $\text{cm}^{-1}$  in OND HCl are shifted by  $\sim 17.36 \text{ cm}^{-1}$  and  $\sim 11$  to 40  $\text{cm}^{-1}$  which is due to purification of hydrochloride form of drug. Strong bond of phenyl molecule was observed in EC (Figure 5.1 c) at 579.18  $\text{cm}^{-1}$ , 880.44  $\text{cm}^{-1}$  and 918.78  $\text{cm}^{-1}$ . At 1059.18, 1112.60  $\text{cm}^{-1}$  C-OH stretching was present and at 1381.17  $\text{cm}^{-1}$  a medium CH<sub>3</sub> bend was observed. A weak aldehyde

stretching was observed at 2875.85  $\text{cm}^{-1}$  and at 2979.03  $\text{cm}^{-1}$ . At 3484.97  $\text{cm}^{-1}$  alcohol stretch, C=O stretch and N-H stretch are also present in EC.

At 2935.66  $\text{cm}^{-1}$  to 3099.61  $\text{cm}^{-1}$  broad O-H band was observed in PVP K-30 which is not overlapped with aliphatic C-H stretching. At 2926.77  $\text{cm}^{-1}$  and 1639.10  $\text{cm}^{-1}$  C-H and C=O stretching vibrations of PVP K-30 were detected. Apart from C-H and C=O stretching, a broad band was also observed at 3403.87  $\text{cm}^{-1}$  which denotes the presence of water (Paradkar *et al.*, 2004). The spectra of HP $\beta$ CD (Figure 5.1e) showed distinct absorption bands at 3401.89  $\text{cm}^{-1}$ , 2932  $\text{cm}^{-1}$ , 1593  $\text{cm}^{-1}$  respectively for O-H stretching vibrations, C-H stretching vibrations and C-C stretching vibration for aromatic ring. Besides, C-H and C-O stretching vibrations were observed at 1156  $\text{cm}^{-1}$  and 1031  $\text{cm}^{-1}$  respectively.

FTIR spectra of HPMC (Figure 5.1f) showed aromatic C-H bending at 610.35  $\text{cm}^{-1}$ . An aromatic C=C bending was observed at 1378.06 and 1457.81  $\text{cm}^{-1}$ . At 2928.28  $\text{cm}^{-1}$  an alkyl C-H stretch was detected. Presence of broad alcohol stretch as well as amine (N-H) stretching was observed at 3457.18  $\text{cm}^{-1}$ .

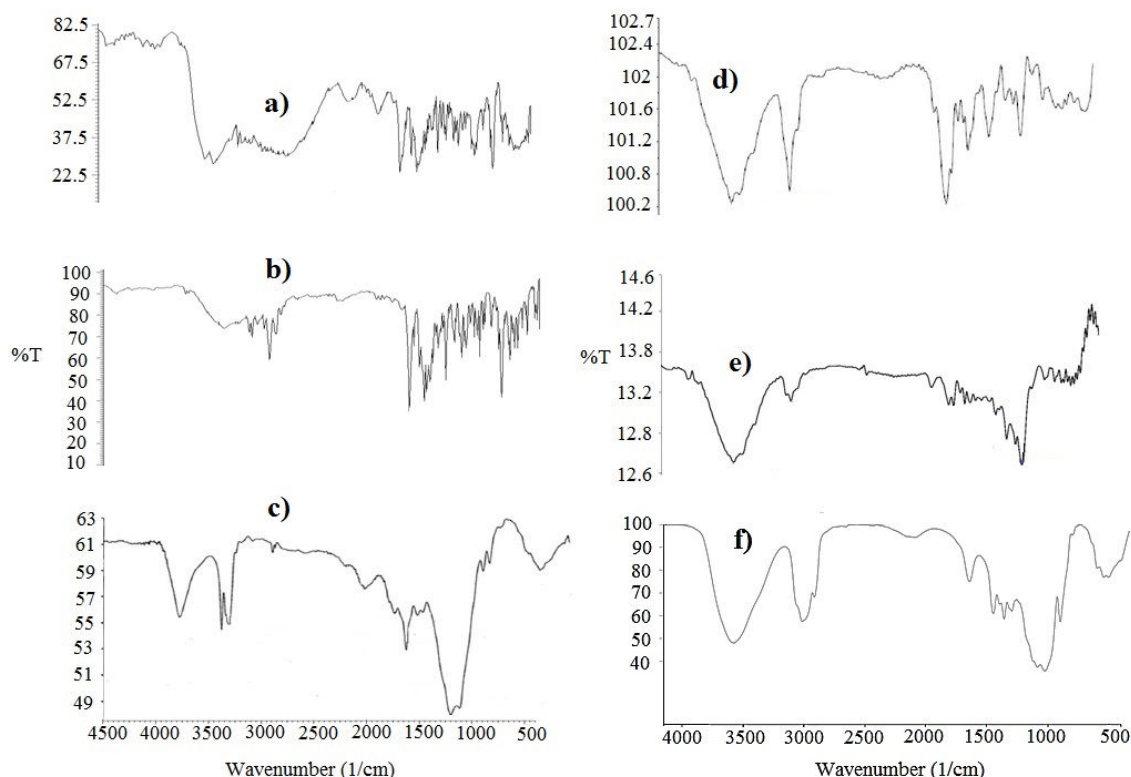


**FIGURE 5.1** - FTIR spectra of a) OND HCl, b) OND c) EC d) PVP K-30 e) HP $\beta$ CD f) HPMC.

The spectra of OND- HP $\beta$ CD SD (1:1, 1:3, 1:5 w/w) based binary system (Figure 5.2 A-C) showed a distinct peaks at 2942, 2935.66 and 2920.60  $\text{cm}^{-1}$  indicated the presence of C-H stretching vibrations. The peaks present at 3319.49, 3299 and 3251.07  $\text{cm}^{-1}$  confirm the presence of O-H band. The frequency present at 3099  $\text{cm}^{-1}$  was absent due to presence of =C-O stretching. Whereas the spectra (Figure 5.2 D-F) of OND-PVP K-30 SD binary system

(1:1, 1:3 and 1:5 w/w) showed C-H stretching at 2947.23, 2945.77 and 2920.12  $\text{cm}^{-1}$  respectively. C=O band were observed at 1621, 1639.10 and 1620.99  $\text{cm}^{-1}$  respectively in case of OND-PVP K-30 (1:1, 1:3 and 1:5 w/w) binary systems. Major frequencies of shifting were observed in both cases. From the above findings it can be concluded that the solid binary systems have satisfactorily formed inclusion complex in between drug and carrier.

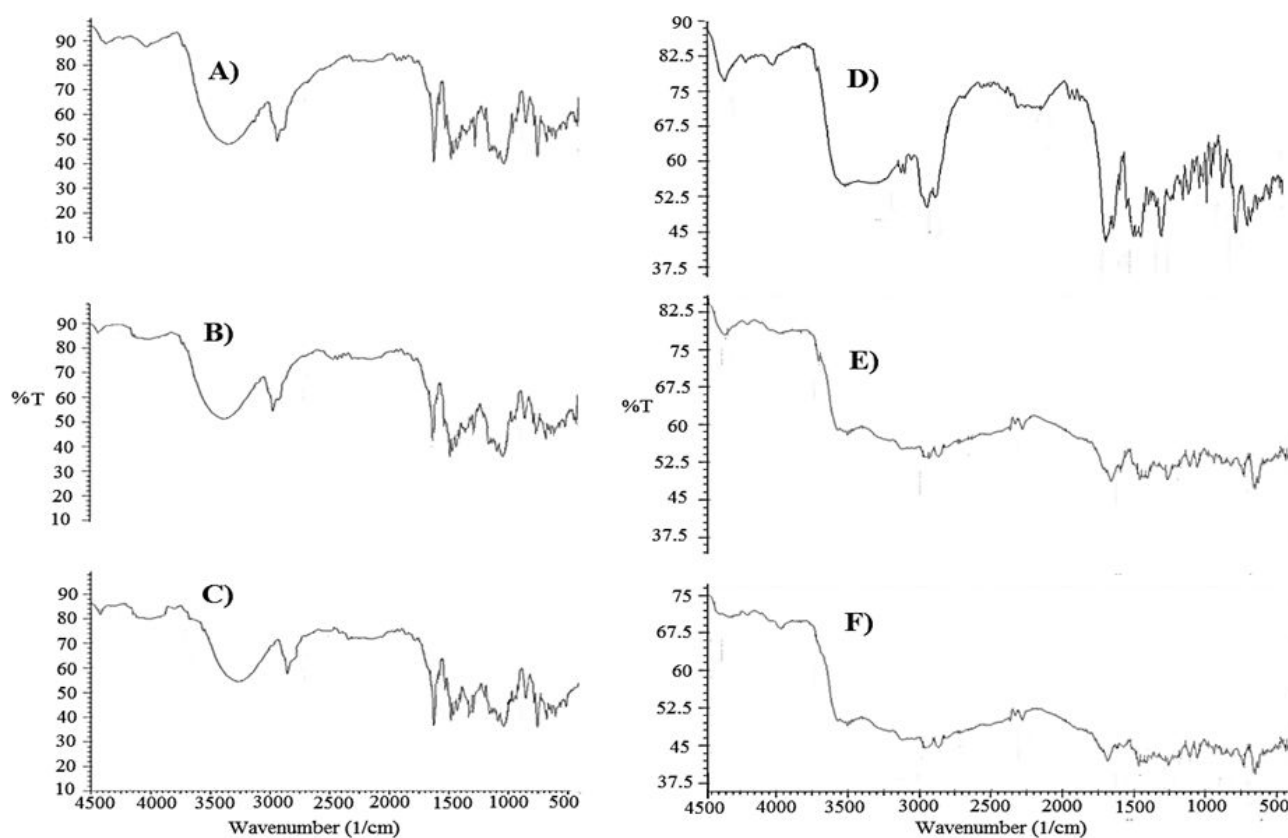


**FIGURE 5.2** - FTIR spectra of a) OND-HP $\beta$ CD 1:1 binary complex; b) OND-HP $\beta$ CD 1:3 binary complex; c) OND-HP $\beta$ CD 1:5 binary complex d) OND-PVP K-30 1:1 binary complex; e) OND-PVP K-30 1:3 binary complex; f) OND-PVP K-30 1:5 binary complex.

FTIR spectra of (Figure 5.3 I) 30% PEG with pure drug loaded patch showed characteristic peak at 1542  $\text{cm}^{-1}$  which denotes the presence of an aromatic group, C=C and ketone (C=O) was present at 1733.69  $\text{cm}^{-1}$ . At 719.6 and 670.2  $\text{cm}^{-1}$ , strong conjugated phenyl group was observed. At 1248  $\text{cm}^{-1}$  and 1343.2  $\text{cm}^{-1}$  a strong C-O-C stretching and NO<sub>2</sub> stretching were observed. Strong CH<sub>3</sub> bending and aromatic ring were observed

at 1458.32 and 1542.53  $\text{cm}^{-1}$ . In case of 40% PEG loaded patch (Figure 5.3 II), NO<sub>2</sub> and C-O-C stretching were shifted approximately 3 and 2  $\text{cm}^{-1}$ . The patches with 30% DBP with plain drug (Figure 5.3 III) showed strong C-O-C stretching and NO<sub>2</sub> stretch at 1241 and 1340.23  $\text{cm}^{-1}$  respectively. Characteristic peaks at 719.6, 870.2 and 1093  $\text{cm}^{-1}$  indicates the presence of strong phenyl group. In case of 40% and 50% DBP loaded patches (Figure 5.3

IV and V) the peaks for phenyl group observed  $\sim 832.32$  and  $820.20\text{ cm}^{-1}$  respectively. Whereas in case of 30% and 40% PEG with SD loaded patches a broader characteristic peak at  $3043.87$  and  $2945.77\text{ cm}^{-1}$  showed presence of C-H stretching (Figure 5.3 VI and VII). The characteristic peak of C=O group present in OND at  $1622\text{ cm}^{-1}$  is shifted to  $1639\text{ cm}^{-1}$  and  $1644.11\text{ cm}^{-1}$ . This indicates the partial

complexation between drug and carrier. In contrast, the characteristic peak (C-H stretching) of OND is absent in 30%, 40% and 50% DBP with SD loaded patches and C=O group present in OND was shifted to  $\sim 79, 90$  and  $92\text{ cm}^{-1}$  respectively in each case (Figure 5.3 VIII-X). This confirms the successful complexation between drug and carrier and also the formation of amorphous matrix.

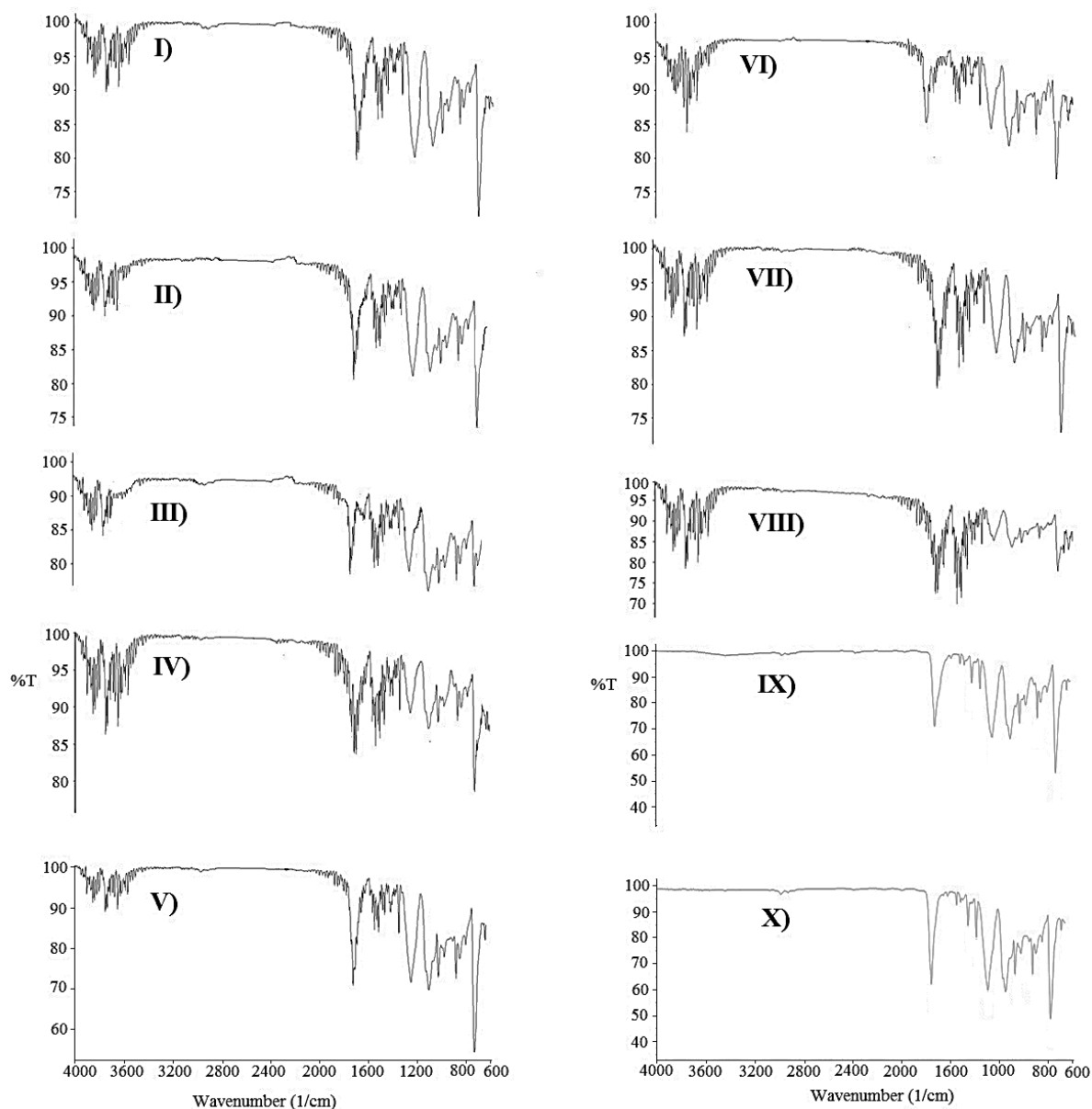


**FIGURE 5.3** - FTIR spectra of **I)** 30% PEG with pure drug loaded patch; **II)** 40% PEG with pure drug loaded patch; **III)** 30% DBP with pure drug loaded patch; **IV)** 40% DBP with pure drug loaded patch; **V)** 50% DBP with pure drug loaded patch, **VI)** 30% PEG with SD loaded patch; **VII)** 40% PEG with SD loaded patch; **VIII)** 30% DBP with SD loaded patch; **IX)** 40% DBP with pure drug loaded patch; **X)** 50% DBP with pure drug loaded patch.

### Differential Scanning Calorimetry (DSC) study

DSC analysis is performed to determine the thermal stability as well as to observe the difference in heat flow between the sample and the reference molecule.

DSC thermogram of OND-HCl and OND (Figure 6 a-b) showed sharp endothermic peak at 186.44 and 233.45°C

respectively (Salem, Lopez, Galan, 2001). The repeated crystallization of OND and removal of impurities cause shifting of endothermic peak from 186.44°C to 233.45°C.

From the DSC thermogram of solid dispersions (Figure 6.1 a-f), it transpires that the peak of OND has almost disappeared. This matter possibly highlights that the drug is entrapped with PVP K-30 and cyclodextrin cavity.

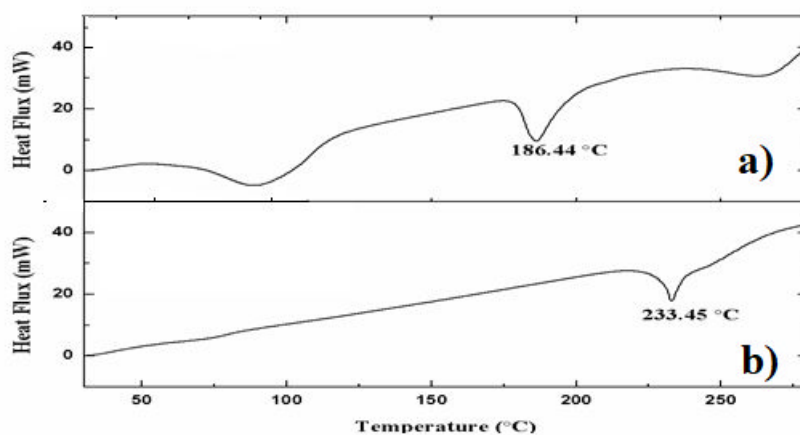


**FIGURE 6** - DSC thermogram of **a)** OND HCl; **b)** OND.

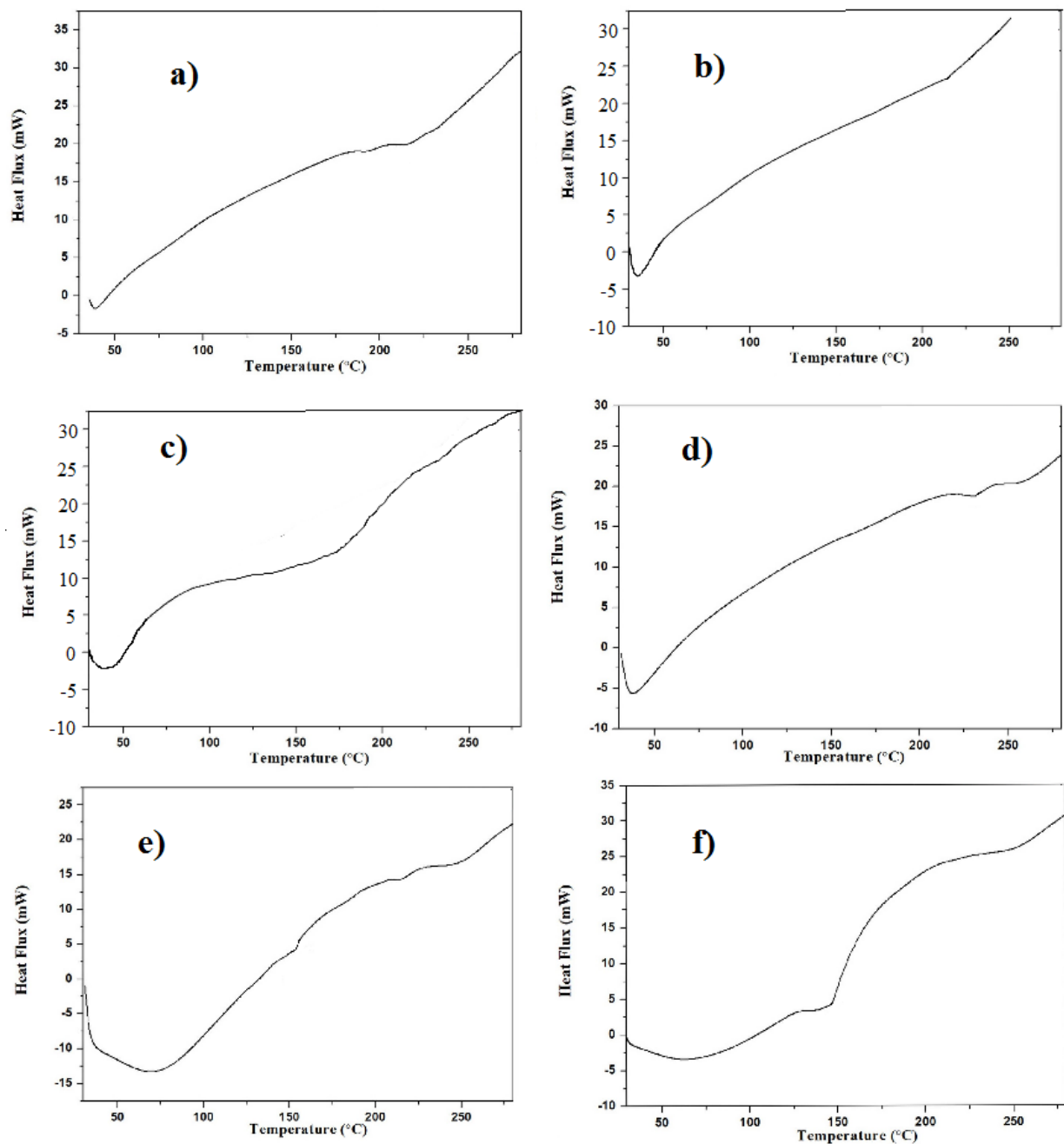


**FIGURE 6.1** - Differential scanning calorimetry study of **a)** OND-PVP K-30 1:1 w/w SD; **b)** OND-PVP K-30 1:3 w/w SD; **c)** OND-PVP K-30 1:5 w/w SD; **d)** OND-HP $\beta$ CD 1:1 w/w SD; **e)** OND-HP $\beta$ CD 1:3 w/w SD; **f)** OND-HP $\beta$ CD 1:5 w/w SD.

#### Scanning electron microscopic analysis (SEM)

The surface morphologies of optimized SD, blank patch, and SD loaded patches have been represented in Figure 7. SEM morphology of OND-PVP K-30 (1:5 w/w) solid binary system prepared by solvent evaporation method

showed rough wrinkled surface (Figure 7 a). This is due to homogeneous dispersion of drug within the carrier.

The surface morphology of blank patch (Figure 7 b) showed rough and irregular surface due to wide distribution of agglomerated molecules of carriers in the matrix.

In 2011 Pattnaik and his co-workers observed the spherulite formation of OND in presence of chloroform as casting solvent. In the present study the pure drug loaded patches with PEG and DBP showed rough matrix but no spherulite formation (Figure 7 c-d). Conversely, in case of SD loaded patches (Figure 7 e-f), amorphous and smooth

matrix was found which confirms the uniform distribution of drug within the PVP K-30 and other polymers. The smoothness of patches is due to the anti-nucleation property of PVP K-30 which abolishes the crystallinity of drug. This fact enlightens that the base form of OND reduces crystallinity in presence of chloroform as casting solvent.

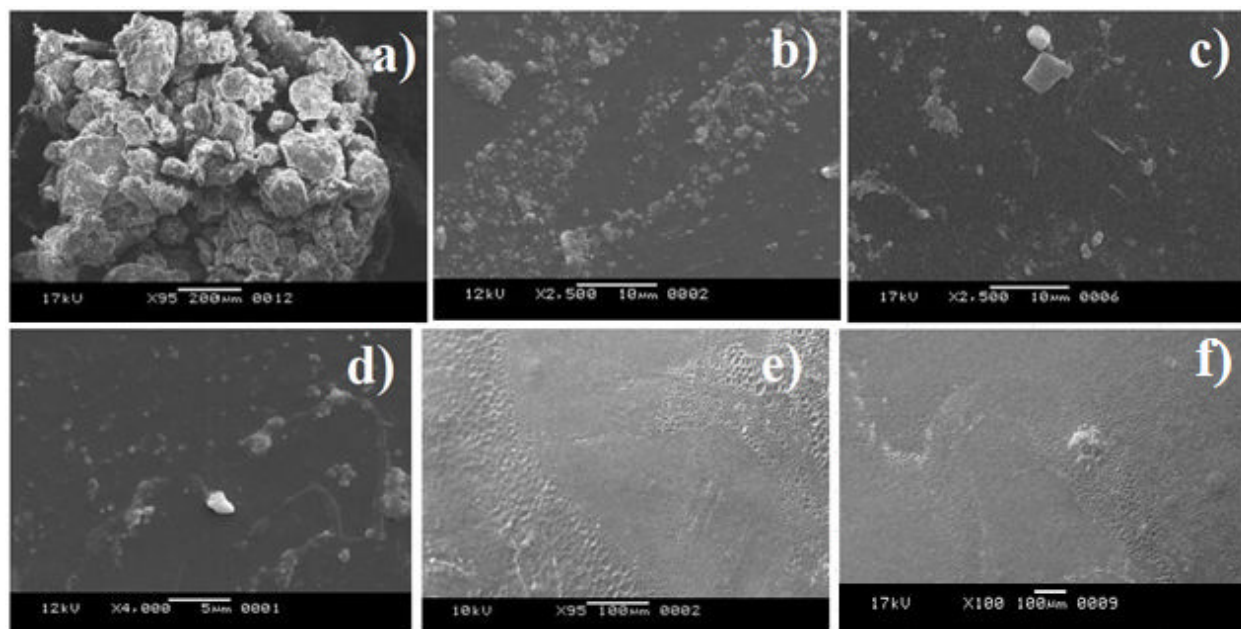


**FIGURE 7** - Scanning electron micrographs of **a)** OND-PVP K-30 1:5 w/w SD; **b)** blank patch; **c)** pure drug loaded patch with 40% PEG; **d)** pure drug loaded patch with 50% DBP; **e)** SD loaded patch with 40% PEG; **f)** SD loaded patch with 50% DBP.

## CONCLUSION

The novelty of the present work is to develop SD loaded transdermal patch which enhances the permeability of OND. After long survey done as yet, no report is available on this current study. Thus, the problems associated with oral dosage form can be overcome and also the bioavailability problem can be minimized. Moreover, it is helpful to overcome the constraint of long term therapy. This matter explored the detailed study on modification of drug and the optimized patch obtained low moisture content (P6\* with DBP,  $1.23 \pm 0.012\%$ ) as compared to PEG ( $2.41 \pm 0.04\%$ ), produced low moisture absorption ( $2.10 \pm 0.031\%$ , P6\* with DBP) in comparison to ( $2.79 \pm 0.046\%$ , P6\* with PEG). Higher permeability coefficient is also found in

case of P6\* with DBP ( $0.12 \pm 0.02$  cm/h). Improved drug content is found in case of DBP loaded P6\* ( $95.33 \pm 3.78\%$ ) as compared to PEG loaded P6\* ( $92.18 \pm 3.63\%$ ). Statistical analysis confirmed the methods statistically significant ( $n < 0.05$ ). The formulations are validated by means of various checkpoint analyses (FTIR, DSC and SEM) to ensure the integrity of the outputs with respect to pharmaceutical drug delivery system. Furthermore, DBP loaded patch (P6\*) indicates more potential antiemetic effect than that of pure drug and P6\* with PEG. From the above findings it is concluded that P6\* with DBP patch is a promising candidate to fight against CINV and PONV.

## CONFLICT OF INTEREST

The authors declare no conflicts of interest.

## ACKNOWLEDGEMENTS

Authors are grateful to the Department of Pharmaceutical Technology, Jadavpur University, Kolkata, India for providing required infrastructure and laboratory facilities.

## FUNDING

In proceeding this research work no specified financial support from funding agencies in private or public sectors obtained.

## REFERENCES

Ahad A, Al-Jenoobi FI, Al-Mohizea AM, Akhtar N, Raish M, Aqil M. Systemic delivery of  $\beta$ -blockers via transdermal route for hypertension. *Saudi Pharm J*. 2015;23(6):587-602.

Ahad A, Aqil M, Kohli K, Sultana Y, Mujeeb M, Ali A. Transdermal drug delivery: the inherent challenges and technological advancements. *Asian J Pharm Sci*. 2010;5(6):276-289.

Alany R. Topical and transdermal formulation and drug delivery. *Pharm Dev Tech*. 2017;22(4):457-457.

Banerjee S, Chattopadhyay P, Ghosh A, Bhattacharya SS, Kundu A, Veer V. Accelerated stability testing of a transdermal patch composed of serine and pralidoxime chloride for prophylaxis against ( $\pm$ )-anatinin a poisoning. *J. Food Drug Anal*. 2014;22(2):264-270.

Bergo P, Sobral PJA. Effects of plasticizer on physical properties of pigskin gelatin films. *Food Hydrocol*. 2006;21(8):1285-1289.

Chien YW. Development of transdermal drug delivery system. *Drug Dev Ind Pharm*. 1987;13(4-5):589-651.

Cilurzo F, Gennari CGM, Minghetti P. Adhesive properties: a critical issue in transdermal patch development. *Expert Opin Drug Deliv*. 2012;9(1):33-45.

Das MK, Ghosal SK. Ex vivo and in vivo evaluation of transdermal formulation of trazodone hydrochloride. *Acta Pol Pharm*. 2008;65(4):481-486.

Das SK, Kahali N, Bose A, Khanam J. Physicochemical characterization and *in vitro* dissolution performance of ibuprofen-Captisol® (sulfobutylether sodium salt of  $\beta$ -CD) inclusion complexes. *J Mol Liq*. 2018;261:239-249.

Desai KGH. Enhanced skin permeation of rofecoxib using topical microemulsion gel. *Drug Dev Res*. 2004;63(1):33-40.

Di L, Kerns EH. Drug like properties: Concepts, Structures design and Methods. 2<sup>nd</sup> Ed. United Kingdom (UK): Academic press, 2016, pp. 497-510.

Elsabee MZ, Abdou ES. Chitosan based edible films and coatings: a review. *Mater Sci Eng C Mater Biol Appl*. 2013;33(4):1819-1841.

Gal A, Nussinovitch A. Plasticizers in the manufacture of novel skin-bioadhesive patches. *Int J Pharm*. 2009;370(1-2):103-109

Ghanghoria R, Kesharwani P, Agashe HB, Jain NK. Transdermal delivery of cyclodextrin-solubilized curcumin. *Drug Deliv Transl Res*. 2013;3(3):272-285.

Guy R, Green MR, Kealey T. Modeling acne *in vitro*. *J Invest Dermatol*. 1996;106(1):176-82.

Hassan N, Khar RK, Ali M, Ali J. Development and evaluation of buccal bioadhesive tablet of an anti-emetic agent ondansetron. *AAPS Pharm Tech*. 2009;10(4):1085-1092.

Higuchi T, Connor's KA. Phase solubility techniques. In: Reilly CN, editor. *Advances in Analytical Chemistry and Instrumentation*. New York: Interscience; 1965. p. 117-212.

Jana S, Ali SA, Nayak AK, Sen KK, Basu SK. Development of topical gel containing aceclofenac-crospovidone solid dispersion by "Quality by Design (QbD)" approach. *Chem Engg Res Des*. 2014;92(11):2095-2105.

Kahali N, Khanam J. A novel HPLC method validation based on analytical techniques of metoclopramide benzamide derivative (Metoclopramide base) and its determination from solid dispersion by solvent evaporation method. *J App Pharm Sci*. 2018;8(2):18-26.

Kahali N, Khanam J, Ghosh N. An attempt to enhance solubility of metoclopramide base by Solid dispersion strategy and its application on development of Transdermal device. *Brazilian J Pharm Sci*. 2021;57:1-22.

Kalimuthu Y, Khanam J. Enhancement of carvedilol solubility by solid dispersion technique using cyclodextrins, water soluble polymers and hydroxyl acid. *J Pharm Biomed Anal*. 2014;96:10-20.

Kandavilli S, Nair V, Panchagnula R. Polymers in transdermal drug delivery systems. *Pharm Tech*. 2002;26:62-81.

Kathe K, Kathpalia H. Film forming systems for topical and transdermal drug delivery. *Asian J Pharm Sci*. 2017;12(6):487-497.

Kaur IP, Geetha TM, Kakkar V. Treatment of skin cancer using sesamol-loaded solid lipid nanoparticles. In: Souto EB, editor. *Lipid nanocarriers in cancer diagnosis and therapy*. 1<sup>st</sup> ed. United Kingdom (UK): A Smithers Group Company. 2011. p. 510-526.

- Khan S, Kataria P, Nakhat P, Yeole P. Taste Masking of ondansetron hydrochloride by polymer carrier system and formulation of rapid-disintegrating tablets. *AAPS Pharm Tech.* 2007;8(2):1-7.
- Loftsson T, Masson M. Cyclodextrins in topical drug formulations: theory and practice. *Int J Pharm.* 2001;225(1-2):15-30.
- Minghetti P, Cilurzo F, Montanari L. Evaluation of adhesive properties of patches based on acrylic matrices. *Drug Dev Ind Pharm.* 1999; 25(1): 1-6.
- Moldoveanu S, David V. Phase transfer in sample preparation. *Modern sample preparation for chromatography.* Amsterdam: The Netherlands. 2015. p. 3-446.
- Mukherjee B, Mahapatra S, Gupta R, Patra B, Tiwari A, Arora P. A comparison between povidone-ethylcellulose and povidone-eudrajit transdermal dexamethasone matrix patches based on *in vitro* skin permeation. *Eur J Pharm Biopharm.* 2005;59(3):475-483.
- Palem CR, Battu SK, Maddineni S, Gannu R, Repka MA, Yamsani MR. Oral transmucosal delivery of domperidone from immediate release films produced via hot-melt extrusion technology. *Pharm Dev Technol.* 2013;18(1):186-195.
- Paradkar A, Ambike AA, Jadhav KB, Mahadik KR. Characterization of curcumin-PVP solid dispersion obtained by spray drying. *Int J Pharm.* 2004;271(1-2):281-286.
- Patel DP, Setty CM, Mistry GN, Patel SL, Patel TJ, Mistry PC, et al. Development and evaluation of ethyl cellulose-based transdermal films of furosemide for improved *In Vitro* skin permeation. *AAPS Pharm Tech.* 2009;10(2):437-442.
- Patil H, Tiwari RV, Upadhye SB, Vladyka RS, Repka MA. Formulation and development of pH-independent/dependent sustained release matrix tablets of ondansetron HCl by a continuous twin-screw melt granulation process. *Int J Pharm.* 2015;496(1):33-41.
- Pattnaik S, Swain A, Mallick S, Lin Q. Effect of casting solvent on crystallinity of ondansetron in transdermal films. *Int J Pharm.* 2011;406(1-2):106-110.
- Prajapati ST, Patel CG, Patel, CN. Formulation and evaluation of transdermal patch of repaglinide. *ISRN Pharm.* 2011;2011:1-9.
- Prausnitz MR, Langer R. Transdermal drug delivery. *Nat Biotechnol.* 2008;26(11):1261-1268.
- Puri A, Bhattacharjee SA, Zhang W, Clark M, Singh ON, Doncel GE, et al. Development of a transdermal delivery system for tenofovir alafenamide, a prodrug of tenofovir with potent antiviral activity against HIV and HBV. *Pharmaceutics.* 2019;11(173):1-29.
- Rao PR, Diwan PV. Permeability studies of cellulose acetate free films for transdermal use: influence of plasticizers. *Pharm Acta Helv.* 1997;72(1):47-51.
- Ravikumar R, Ganesh M, Ubaidulla U, Choi EY, Jang HT. Preparation, characterization, and *in vitro* diffusion study of nonwoven electrospun nanofiber of curcumin-loaded cellulose acetate phthalate polymer. *Saudi Pharm J.* 2017;25(6):921-926.
- Rogers TL, Hypromellose: Rowe RC, Sheskey PJ, Quinn ME, (Eds.), *Handbook of Pharmaceutical Excipients.* London: Pharmaceutical Press. 2009. p. 326-329.
- Salem II, Lopez JMR, Galan AC. Ondansetron Hydrochloride. In: Brittain HG editor. *Analytical Profiles of Drug Substances and Excipients.* U.S.A: Elsevier Academic press. 2001. p. 301-338.
- Schmook FP, Meingassner JG, Billich A. Comparison of human skin or epidermis models with human and animal skin in *in-vitro* percutaneous absorption. *Int J Pharm.* 2001;215(1-2):51-60.
- Singh A, Bali A. Formulation and characterization of transdermal patches for controlled delivery of duloxetine hydrochloride. *J Anal Sci Tech.* 2016;25:1-13.
- Soliman SM, Malak NSA, El Gazayerly ON, Abdel Rahim, AA. Preparation of celecoxib solid dispersions for dermal application: *in vitro* characterization and skin irritation test. *J Drug Del Sci Tech.* 2011; 21(6):509-516.
- Subedi RK, Oh SY, Chun MK, Choi HK. Recent Advances in Transdermal Drug Delivery. *Arch Pharm Res.* 2010;33:339-351.
- Suthar RM, Chotai NP, Patel HK, Patel SR, Shah DD, Jadeja MB. *In vitro* dissolution enhancement of ondansetron by solid dispersion in superdisintegrants. *Dissol Technol.* 2013;20(4):34-38.
- Thakur G, Singh A, Singh I. Formulation and evaluation of transdermal composite films of chitosan-montmorillonite for the delivery of curcumin. *Int J Pharm Investig.* 2016;6(1):23-31.
- Walters KA, *Transdermal drug delivery systems:* Swarbrick K, Boylan JC, (Eds.). *Encyclopedia of Pharmaceutical Technology.* New York, Marcel Dekker, 1999. p. 306-320.
- Wu C, Williams III RO, O'Donnell K, Dong Y, Lang B, Li H, et al. Formulation and delivery of improved amorphous fenofibrate solid dispersions prepared by thin film freezing. *Eur J Pharm Biopharm.* 2012;82(3):534-544.
- Zheng L, Reza F. Influence of colloidal silicon dioxide on gel strength, robustness, and adhesive properties of diclofenac gel formulation for topical application. *AAPS Pharm Tech.* 2014;16(3):636-644.

Received for publication on 28<sup>th</sup> March 2020

Accepted for publication on 19<sup>th</sup> November 2020